STANFORD
AERONAUTICS &
ASTRONAUTICS

A Universal Velocity Profile for Wall Bounded Flows

Summary of Lectures 1, 2 and 3

The first three lectures will be focused on wall-bounded flows. This research is quite recent. Most of it has been carried out since 2019. The latest work is not yet published.

Lecture 1 - In this lecture a useful mixing length model for wall bounded flows will be described. The corresponding Universal Velocity Profile (UVP) accurately approximates pipe, channel and boundary layer flows including flows with pressure gradients. The velocity profile is uniformly valid from the wall to the free stream at all Reynolds numbers. A modified Clauser pressure gradient parameter is derived which correlates two of the model parameters.

Lecture 2 - The inherent dependence of the UVP on Reynolds number, extended to include the effect of pressure gradient, enables it to be used as the basis of a new integral method for solving the Kármán equation for a wide variety of attached flows. Since the velocity profile is a known integrable function of the pressure gradient parameter, the time required to compute the viscous drag of a body such as an airfoil is independent of the Reynolds number and so there is no practical upper limit to the Reynolds number that can be evaluated. The application of the UVP to rough-wall pipe flow is also described. The rough-wall version of the UVP approximates rough-wall pipe data to a high level of accuracy comparable to the smooth-wall case.

Lecture 3 - While the agreement between the UVP and DNS and experimental data is generally very good, there is disagreement between the UVP and velocity derivative data from DNS near the wall. Over the past year, a new wall damping function has been derived that substantially improves the agreement while at the same time reducing the number of parameters in the UVP model from 5 to 4 for pipes and channels and from 4 to 3 for boundary layers. The variation in model parameter values from case to case is also reduced, especially for boundary layer flows.

The main goal of the first three lectures is to demonstrate useful features of the UVP and to support the case for carrying out moderate Reynolds number DNS of boundary layers with pressure gradients.

Open Access links to the relevant references at JFM and Physics of Fluids are on my website at https://web.stanford.edu/~cantwell/

PDFs of these lectures can also be found on my website at https://web.stanford.edu/~cantwell/AA218_Course_Material/ in a folder labeled ‘China Lectures May 2025’

Brian Cantwell
Stanford University
May 12, 2025

Beihang University, Beijing China May 7, 2025, to June 4, 2025

STANFORD
AERONAUTICS &
ASTRONAUTICS

The turbulent boundary layer mean velocity profile

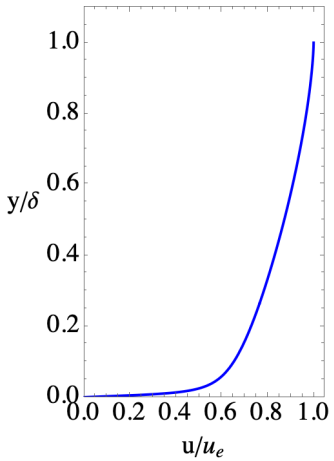

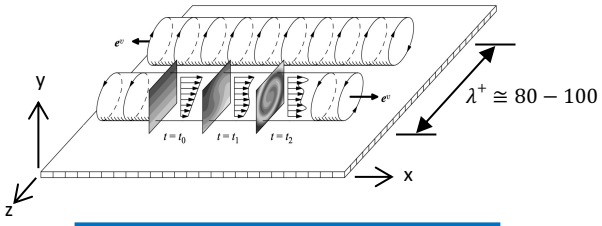

From: D. Chung and D.I. Pullin LES and wall modeling of turbulent channel flow. JFM vol 631, 2009 – Fig 2

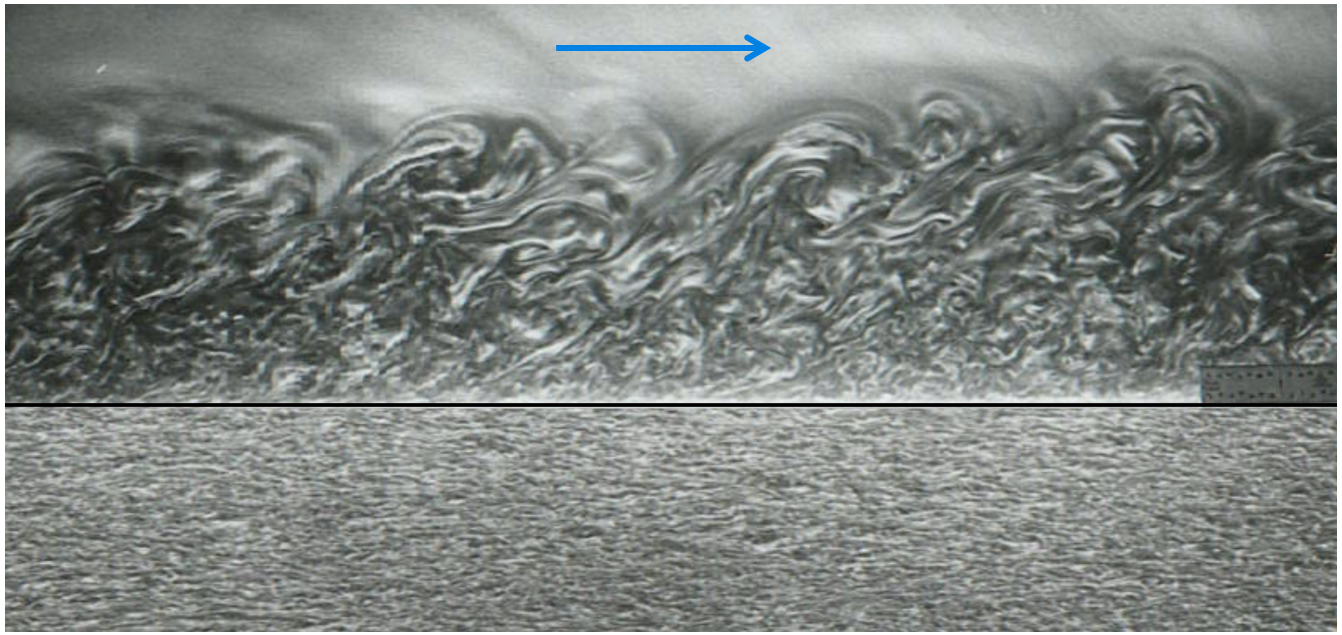

Camera setup

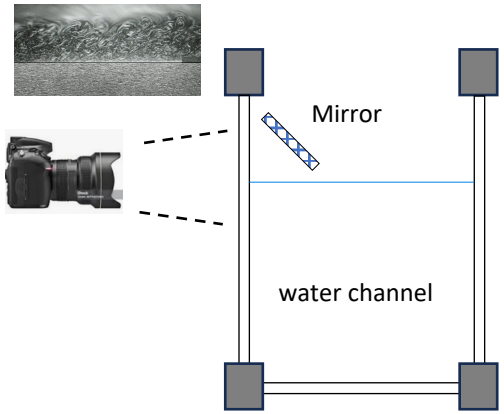

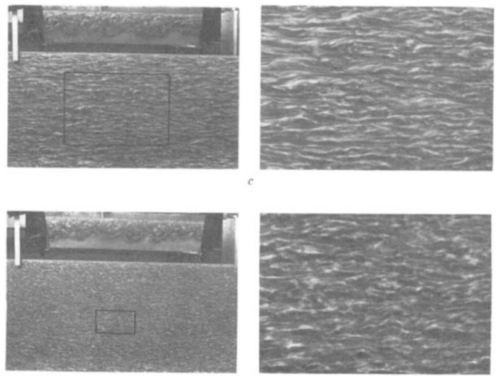

Turbulent boundary layer wall variables y^+ and u^+ and the friction Reynolds number R_τ

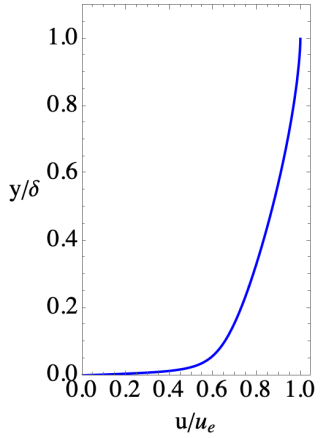

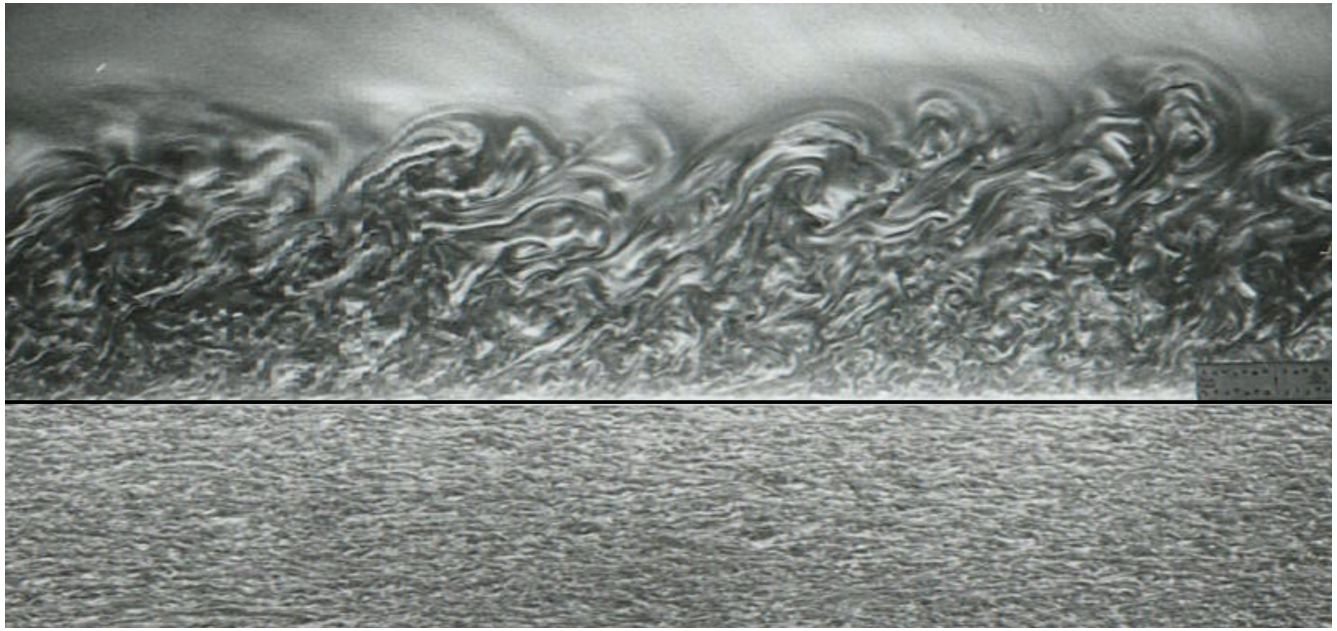

$$\tau_w = \mu \left.\frac{\partial U}{\partial y}\right|_{y=0} \qquad u_\tau = \sqrt{\frac{\tau_w}{\rho}}$$

$$y^+ = \frac{y u_\tau}{\nu} \qquad u^+ = \frac{u}{u_\tau}$$

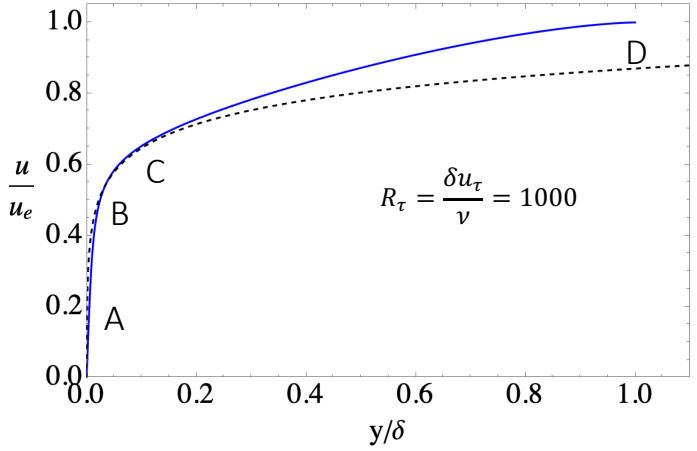

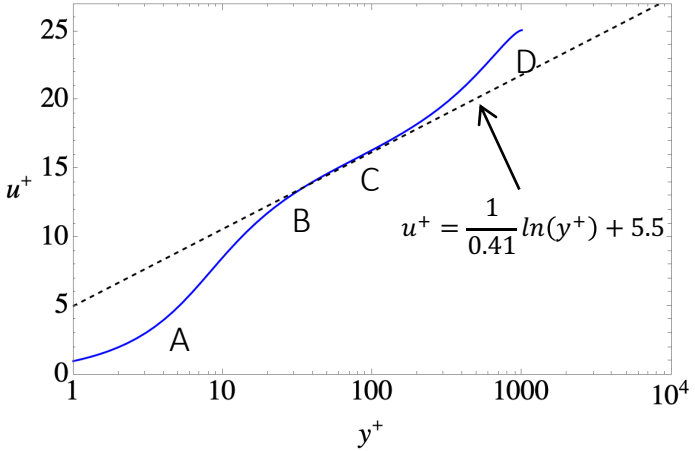

$$R_\tau = \frac{\delta u_\tau}{\nu} = \delta^+$$

$$\frac{y}{\delta} = \frac{y^+}{R_\tau}$$

STANFORD
AERONAUTICS & ASTRONAUTICS

Classical wall-wake formulation

Coles (1956) recommends
$W = 2\sin^2\left(\frac{\pi}{2}\frac{y}{\delta}\right)$
$\kappa = 0.41$, $C = 5.5$
for $dPe/dx = 0$, $\Pi = 0.62$

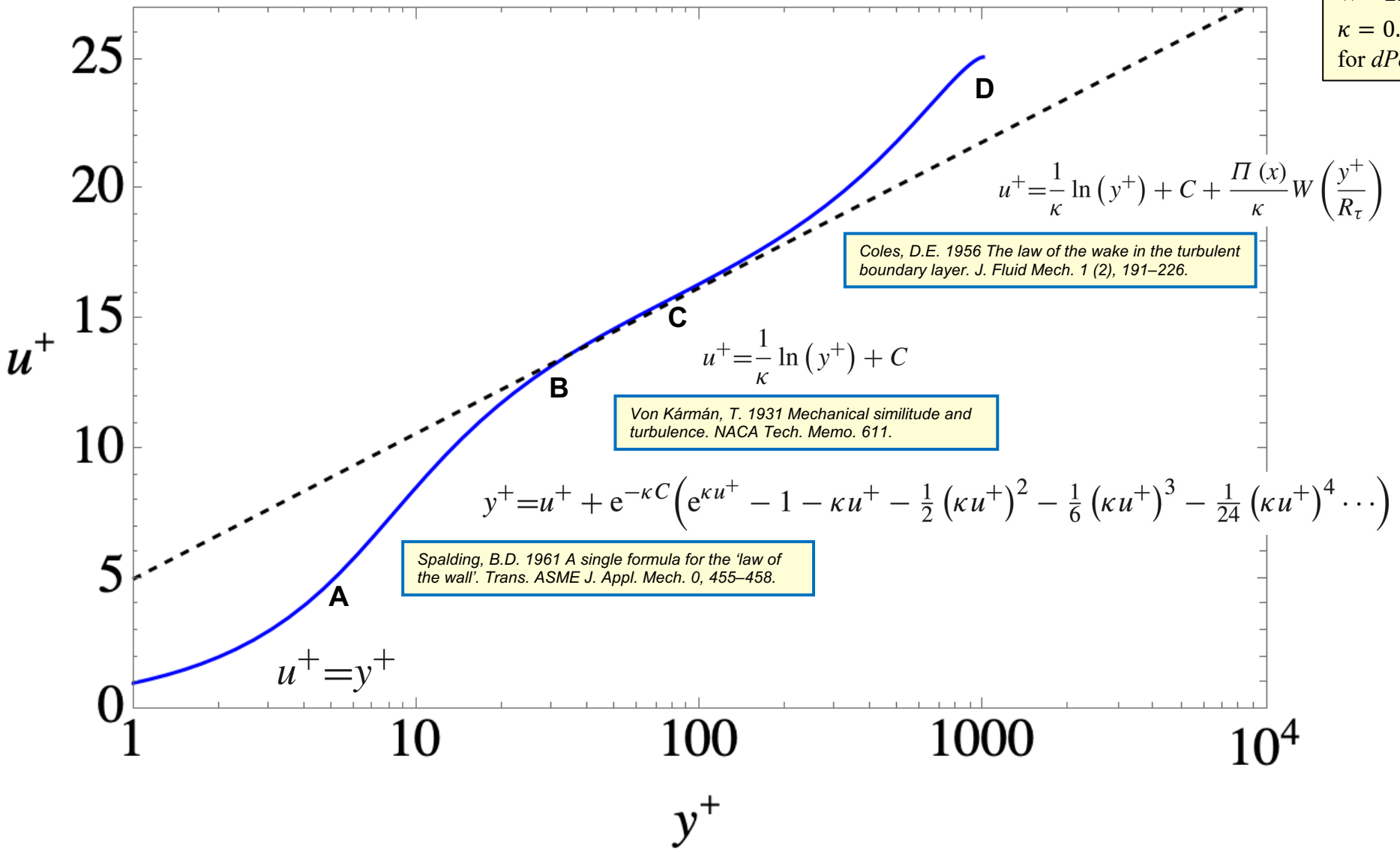

Coles, D.E. 1956 The law of the wake in the turbulent boundary layer. J. Fluid Mech. 1 (2), 191–226.

Von Kármán, T. 1931 Mechanical similitude and turbulence. NACA Tech. Memo. 611.

Spalding, B.D. 1961 A single formula for the 'law of the wall'. Trans. ASME J. Appl. Mech. 0, 455–458.

Reynolds number dependence of the mean velocity profile

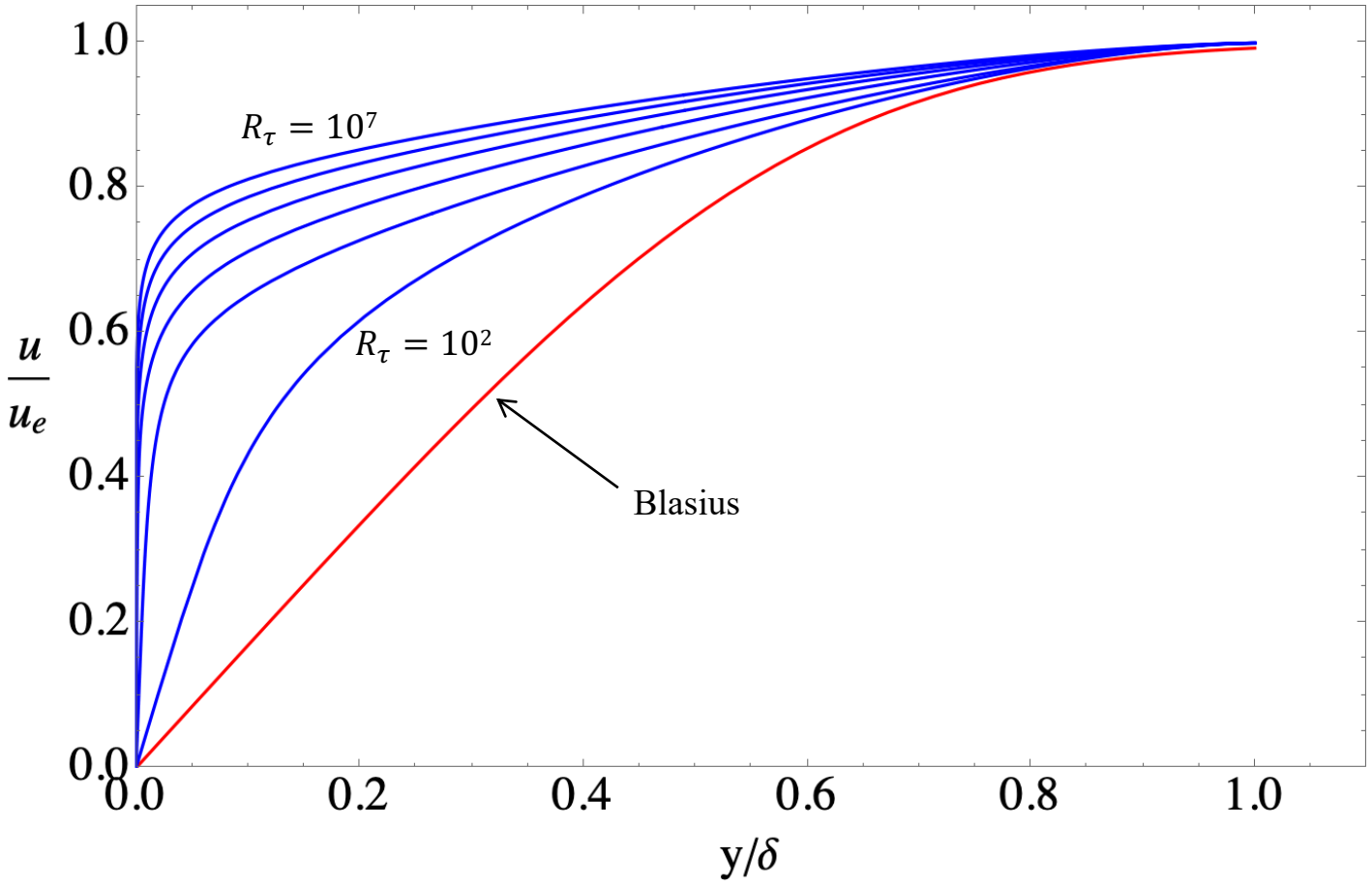

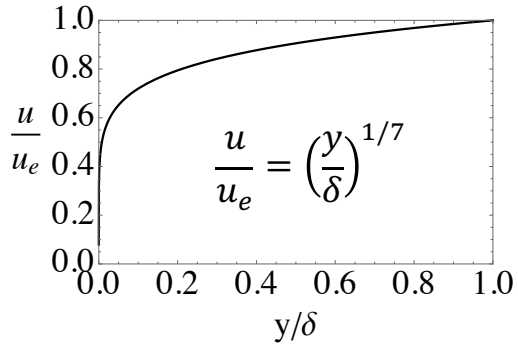

A common approximation is to use a 1/7 power law profile, but this fails to capture the most important property of the turbulent boundary layer which is the dependence of the profile shape on the Reynold number.

The thickness δ is arbitrarily defined. Typically, $\delta_{0.99}$ or $\delta_{0.995}$ is used where $u(\delta)=0.99u_e$ or $u(\delta)=0.995\ u_e$.

Problems with the wall-wake profile

1) Separate layers need to be matched

2) Discontinuity in du/dy at the outer edge of the boundary layer due to the ln(y^+) term

3) Profile is not connected to any model of the turbulent shear stress

4) The profile is not accurate at low Reynolds numbers

5) The profile is accurate at high Reynolds numbers but the value of "high Reynolds number" is not specified.

The Princeton Superpipe (PSP) Facility

Zagarola, M. V. & Smits, A. J. 1998 Mean-flow scaling of turbulent pipe flow. J. Fluid Mech. 373, 33–79.

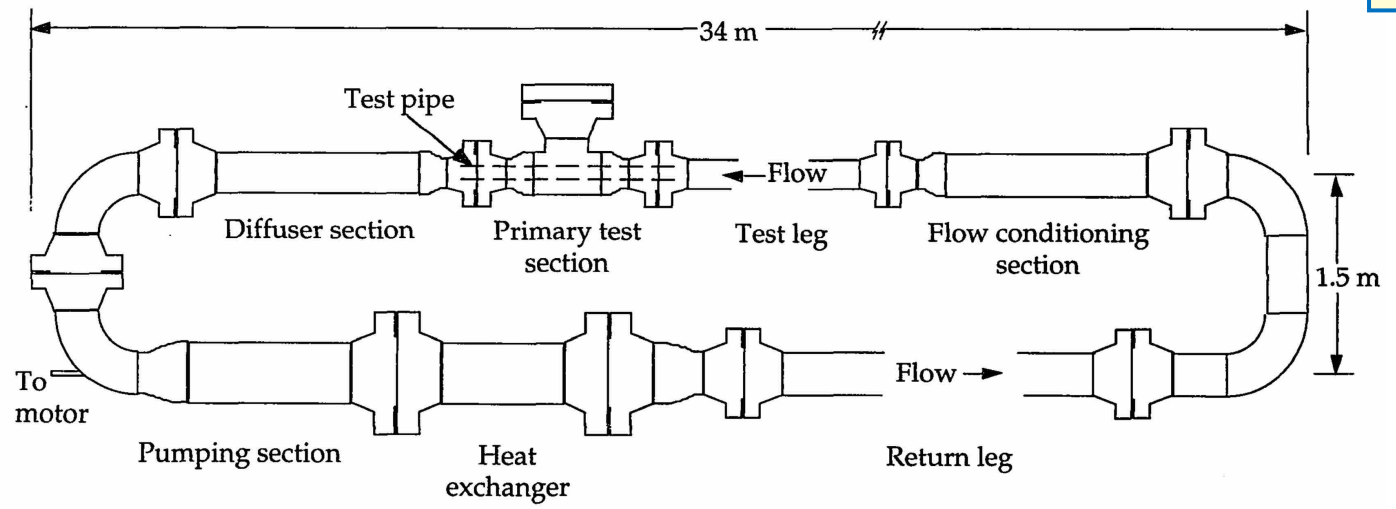

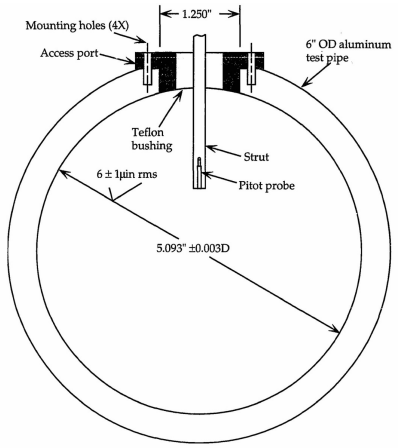

ZAGAROLA, M. V. 1996 Mean-flow scaling of turbulent pipe flow. Doctoral Dissertation, Princeton University.

Pitot tube diameter = 0.9mm

MCKEON, B. J. 2003 High Reynolds number turbulent pipe flow. Doctoral Dissertation, Princeton University.

Pitot tube diameter = 0.3mm

26 cases

$19639 < R_e < 20{,}088{,}000$

$851 < R_\tau < 530{,}000$

$23 < {}^{u_0}/_{u_\tau} < 38$

$$R_e = \frac{u_0 R}{\nu}$$

Pipe Flow

$$\eta = \frac{r}{\delta}$$
$$U = \frac{u}{u_0}$$
$$R_e = \frac{u_0 \delta}{\nu}$$

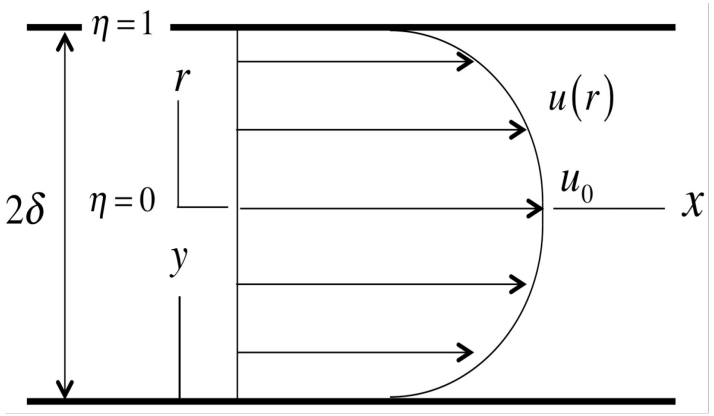

Laminar solution

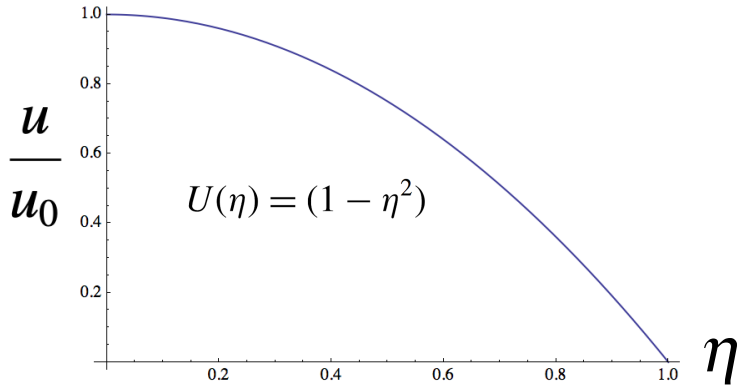

Balance between shear stress and the pressure gradient

$$\frac{1}{r}\frac{\mathrm{d}}{\mathrm{d}r}(r(\overline{u'v'})) - \nu\frac{1}{r}\frac{\mathrm{d}}{\mathrm{d}r}\left(r\frac{\mathrm{d}u}{\mathrm{d}r}\right) + \frac{1}{\rho}\frac{\partial p(x,\, r)}{\partial x} = 0$$

Reynolds shear stress

viscous shear stress

pressure gradient

Neglect possible dependence of the mean pressure on radius.

Notation

$$\eta = \frac{r}{\delta}$$

$$U = \frac{u}{u_0}$$

$$R_e = \frac{u_0 \delta}{\nu}$$

$$\tau_w = \mu \left. \frac{\mathrm{d}u}{\mathrm{d}r} \right|_{r=\delta}$$

$$C_f = -\frac{2\tau_w}{\rho u_0^2} = 2\frac{u_\tau^2}{u_0^2}$$

$$\frac{1}{\rho}\frac{\mathrm{d}p(x,r)}{\mathrm{d}x} = \frac{2}{\delta}\left(\frac{\tau_w}{\rho}\right)$$

$$\tau = -\frac{\overline{u'v'}}{{u_0}^2}.$$

$$u_\tau = \left(-\frac{\tau_w}{\rho}\right)^{1/2}$$

$$R_\tau = \frac{\delta u_\tau}{\nu}$$

$$u^+ = \frac{u}{u_\tau} = \frac{R_e}{R_\tau}U$$

$$y = \delta - r$$

$$y^+ = \frac{y u_\tau}{\nu} = (1-\eta)R_\tau$$

$$\tau^+ = \frac{\overline{u'v'}}{u_\tau^2} = -\left(\frac{R_e}{R_\tau}\right)^2 \tau$$

Pipe Flow – wall variables

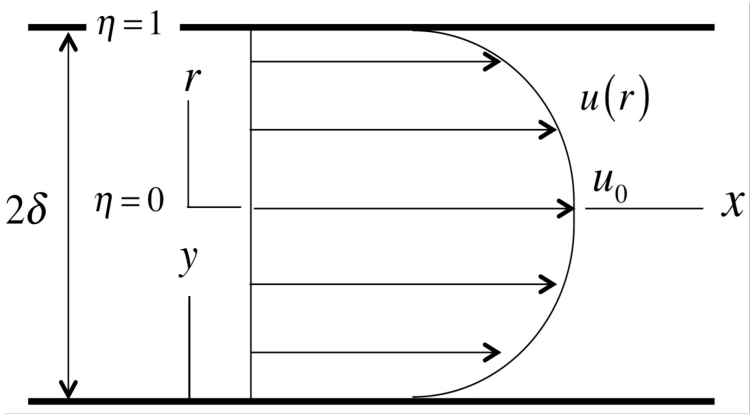

Integrate the governing equation once and apply the centerline boundary condition *dU/dr = 0* at *r = 0*. Express the first order governing equation in terms of wall variables.

$$\tau^+ + \frac{\mathrm{d}u^+}{\mathrm{d}y^+} - \left(1 - \frac{y^+}{R_\tau}\right) = 0$$

$$u^+ = \frac{u}{u_\tau} \qquad y^+ = \frac{yu_\tau}{\nu} \qquad \tau^+ = \frac{\overline{u'v'}}{u_\tau^2}$$

Laminar solution in wall variables

$$u^+_{laminar} = y^+\left(1 - \frac{y^+}{2R_\tau}\right)$$

$$C_{f_{laminar}} = \frac{8}{R_\tau{}^2}$$

$$u_\tau = \left(-\frac{\tau_w}{\rho}\right)^{1/2}$$

$$R_\tau = \frac{\delta u_\tau}{\nu}$$

Note

$$\frac{u_0}{u_\tau} \equiv \frac{R_e}{R_\tau} \equiv \sqrt{\frac{2}{C_f}}$$

STANFORD
AERONAUTICS & ASTRONAUTICS

Mixing length model for the turbulent shear stress

$$\tau^+ = \left(\lambda(y^+)\frac{du^+}{dy^+}\right)^2$$

Prandtl 1934

The first order governing equation becomes a quadratic equation in the derivative of the mean velocity

$$\left(\frac{du^+}{dy^+}\right)^2 + \frac{1}{\lambda(y^+)^2}\frac{du^+}{dy^+} - \frac{1}{\lambda(y^+)^2}\left(1 - \frac{y^+}{R_\tau}\right) = 0$$

Take the positive root

$$\frac{du^+}{dy^+} = -\frac{1}{2\lambda(y^+)^2} + \frac{1}{2\lambda(y^+)^2}\left(1 + 4\lambda(y^+)^2\left(1 - \frac{y^+}{R_\tau}\right)\right)^{1/2}$$

Remove the singularity at $\lambda = 0$

$$\frac{du^+}{dy^+} = \frac{2\left(1 - \frac{y^+}{R_\tau}\right)}{1 + \left(1 + 4\lambda\,(y^+)^2\left(1 - \frac{y^+}{R_\tau}\right)\right)^{1/2}}$$

STANFORD
AERONAUTICS &
ASTRONAUTICS

Define a new mixing length function

$$\lambda(y^+) = \frac{ky^+(1 - e^{-(y^+/a)^m})}{\left(1 + \left(\frac{y^+}{bR_\tau}\right)^n\right)^{1/n}}$$

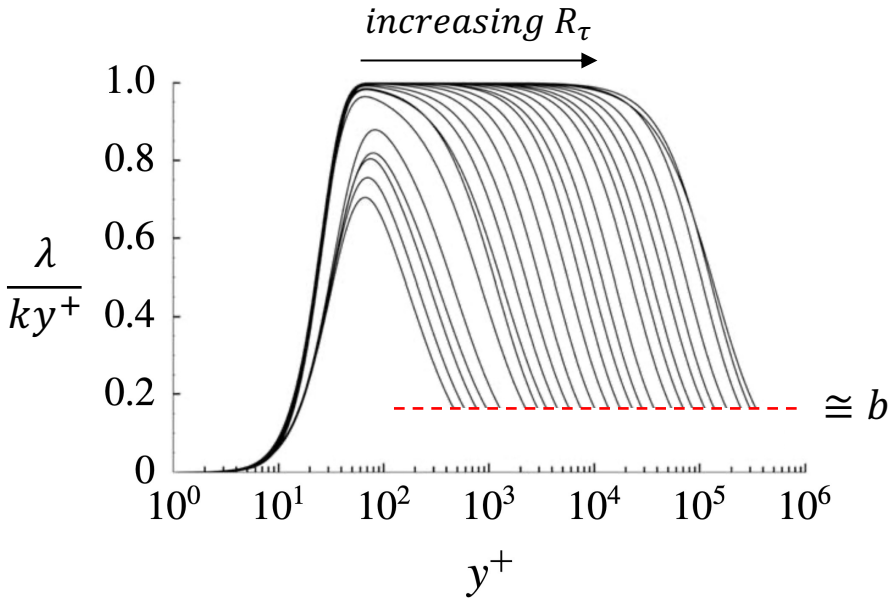

k - essentially the Karman constant.

a - wall damping length scale similar to the van Driest length.

m - exponent that, along with *a*, governs the shape and thickness of the near wall profile.

b - length scale proportional to the distance above the wall of the beginning of the outer layer.

n - exponent that, along with *b*, controls the transition of the profile to the wake function.

Later we will see that, for boundary layers, *b* and *n* can be related through a modified Clauser parameter β_c.

STANFORD AERONAUTICS & ASTRONAUTICS

The Universal Velocity Profile (UVP) - Integrate the velocity derivative from the wall

The velocity profile is uniformly valid from the wall to the pipe centerline at all Reynolds numbers.

$$u^+(k,a,m,b,n,R_\tau,y^+) = \int_0^{y^+} \frac{2\left(1-\frac{s}{R_\tau}\right)}{1+\left(1+4\lambda^2\left(1-\frac{s}{R_\tau}\right)\right)^{1/2}} ds$$

$$\lambda(y^+) = \frac{ky^+(1-\mathrm{e}^{-(y^+/a)^m})}{\left(1+\left(\frac{y^+}{bR_\tau}\right)^n\right)^{1/n}}$$

The boundary layer friction law is generated by evaluating the UVP at $y^+ = R_\tau$

$$\frac{u_e}{u_\tau} = \int_0^{R_\tau} \frac{2\left(1-\frac{s}{R_\tau}\right)}{1+\left(1+4\lambda^2\left(1-\frac{s}{R_\tau}\right)\right)^{1/2}} ds$$

The velocity profile reduces to the laminar solution in the limit of zero Reynolds number independent of the choice of λ.

$$\lim_{R_\tau\to 0} \int_0^{y^+} \frac{2\left(1-\frac{s}{R_\tau}\right)}{1+\left(1+4\lambda^2\left(1-\frac{s}{R_\tau}\right)\right)^{1/2}} ds = y^+\left(1-\frac{y^+}{2R_\tau}\right)$$

$$\lim_{R_\tau\to 0} C_f = \frac{2}{\left(\lim_{R_\tau\to 0}\int_0^{R_\tau} \frac{2\left(1-\frac{s}{R_\tau}\right)}{1+\left(1+4\lambda^2\left(1-\frac{s}{R_\tau}\right)\right)^{1/2}} ds\right)^2} = \frac{8}{{R_\tau}^2}$$

STANFORD AERONAUTICS & ASTRONAUTICS

Determination of best fit model parameters

Minimize G with respect to k, a, m, b, n

$$G = \sum_{i=1}^{N} (u^+(k, a, m, b, n, y_i^+) - u_i^+(y_i^+))^2$$

UVP

PSP data

Flow conditions and optimal model parameters for all 26 velocity profiles

PSP #	p_d mm	u_τ	R_τ	R_e	$\bar{R}_e$	k	a	m	b	n	u_0/u_τ	$u^+_{\text{rms error}}$	$u^+_{\max error}$	$u^+_{\min error}$
1	0.9	0.2089	850.947	19639.	15789.	0.459526	25.801	1.28798	0.299588	1.23686	23.0788	0.152301	0.538874	-0.139258
2	0.9	0.2683	1090.56	25818.	20864.	0.45944	25.7568	1.28759	0.293575	1.24395	23.6738	0.116743	0.474895	-0.185527
3	0.9	0.3455	1430.26	34818.	28339.	0.457774	25.7518	1.28734	0.291299	1.24498	24.3436	0.0971337	0.371735	-0.184978
4	0.3	0.432	1824.72	45284.	37173.	0.455477	25.863	1.25214	0.295422	1.18658	24.8171	0.135614	0.344811	-0.128301
5	0.9	0.5641	2344.74	59872.	49406.	0.452669	25.6633	1.29994	0.297001	1.2471	25.5345	0.0807474	0.192072	-0.164053
6	0.3	0.7919	3327.37	87150.	72290.	0.403394	19.7637	1.4964	0.350243	1.33343	26.1918	0.211454	0.682335	-0.287154
7	0.9	1.0065	4124.89	110550.	92715.	0.403106	20.2094	1.61048	0.341454	1.51165	26.8018	0.107034	0.182098	-0.270575
8	0.3	0.4183	5108.56	139380.	116990.	0.400524	19.6565	1.55346	0.353091	1.37315	27.284	0.155725	0.666555	-0.185794
9	0.3	0.5437	6617.44	183270.	154820.	0.406081	19.682	1.61578	0.330602	1.48471	27.6954	0.112958	0.485734	-0.164828
10	0.3	0.7035	8536.62	242050.	205430.	0.405547	19.7355	1.63359	0.32875	1.51099	28.3537	0.0863432	0.387908	-0.137764
11	0.3	0.9003	10 914.4	314810.	268470.	0.406278	19.8188	1.6433	0.322005	1.61863	28.8432	0.0533497	0.155367	-0.114963
12	0.3	0.2423	14 848.9	439790.	376800.	0.405533	19.8187	1.63899	0.317069	1.64829	29.6175	0.0582442	0.0984979	-0.144372
13	0.3	0.323	19 778.3	599100.	515450.	0.405505	19.8541	1.64732	0.323093	1.66532	30.2907	0.0456737	0.0825095	-0.0989688
14	0.3	0.4136	25 278.1	780760.	673100.	0.406013	19.9893	1.6426	0.317063	1.75114	30.8868	0.0411267	0.0582979	-0.156567
15	0.3	0.5411	32 869.1	1038300.	897500.	0.40532	19.8023	1.65305	0.32421	1.66428	31.5881	0.0508534	0.118501	-0.14304
16	0.3	0.7001	42 293.5	1363000.	1181500.	0.406164	19.9961	1.62818	0.307786	1.71916	32.2268	0.0690966	0.175211	-0.12347
17	0.3	0.4721	54 530.6	1785500.	1552500.	0.407998	20.075	1.6311	0.30966	1.73322	32.743	0.0743128	0.259387	-0.106957
18	0.3	0.1759	76 479.8	2558700.	2231100.	0.40993	20.0117	1.65763	0.326951	1.68545	33.4563	0.0885882	0.262977	-0.281911
19	0.3	0.2358	102 200.	3500000.	3056400.	0.409934	19.9569	1.64637	0.317958	1.66433	34.2462	0.0779887	0.228758	-0.17882
20	0.3	0.2147	127 914.	4457300.	3903100.	0.410112	20.0706	1.63716	0.312475	1.64664	34.8458	0.074515	0.211301	-0.192975
21	0.3	0.2782	165 704.	5884200.	5157000.	0.410176	20.0915	1.64094	0.314927	1.6552	35.5102	0.0595818	0.214504	-0.122477
22	0.3	0.3652	216 979.	7813500.	6859500.	0.416118	20.6722	1.58559	0.293151	1.68512	36.0106	0.0706957	0.292235	-0.0989045
23	0.3	0.4821	284 254.	10392000.	9154000.	0.417539	20.673	1.59258	0.294283	1.67078	36.5586	0.058332	0.20287	-0.105169
24	0.9	0.6168	366 972.	13540000.	11989000.	0.418696	20.8983	1.62571	0.306356	1.75128	36.8963	0.0999892	0.155755	-0.269669
25	0.9	0.7571	452 380.	16888000.	14964000.	0.419289	20.8329	1.62031	0.303987	1.73244	37.3313	0.0669581	0.109743	-0.178982
26	0.3	0.9127	530 023.	20088000.	17862000.	0.418993	20.3797	1.64264	0.314469	1.49687	37.9002	0.096876	0.291624	-0.114251

STANFORD
AERONAUTICS &
ASTRONAUTICS

Optimal values of k and a

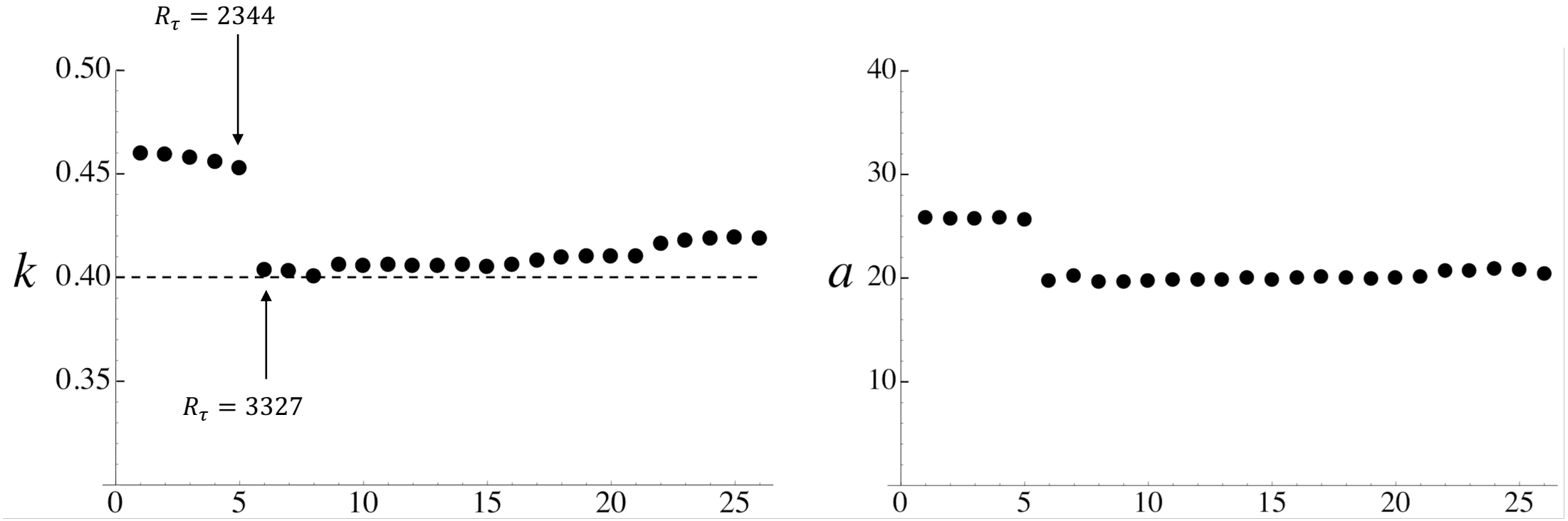

STANFORD
AERONAUTICS &
ASTRONAUTICS

The minimization process is not convex. Alternate values of the model parameters can lead to the same accuracy. This seems to be the case at low and moderate Reynolds numbers but less so at Reynolds numbers above R_τ = 20,000 or so. Experience suggests that at high R_τ the minima may lie very close together in parameter space, but no analysis exists to show this.

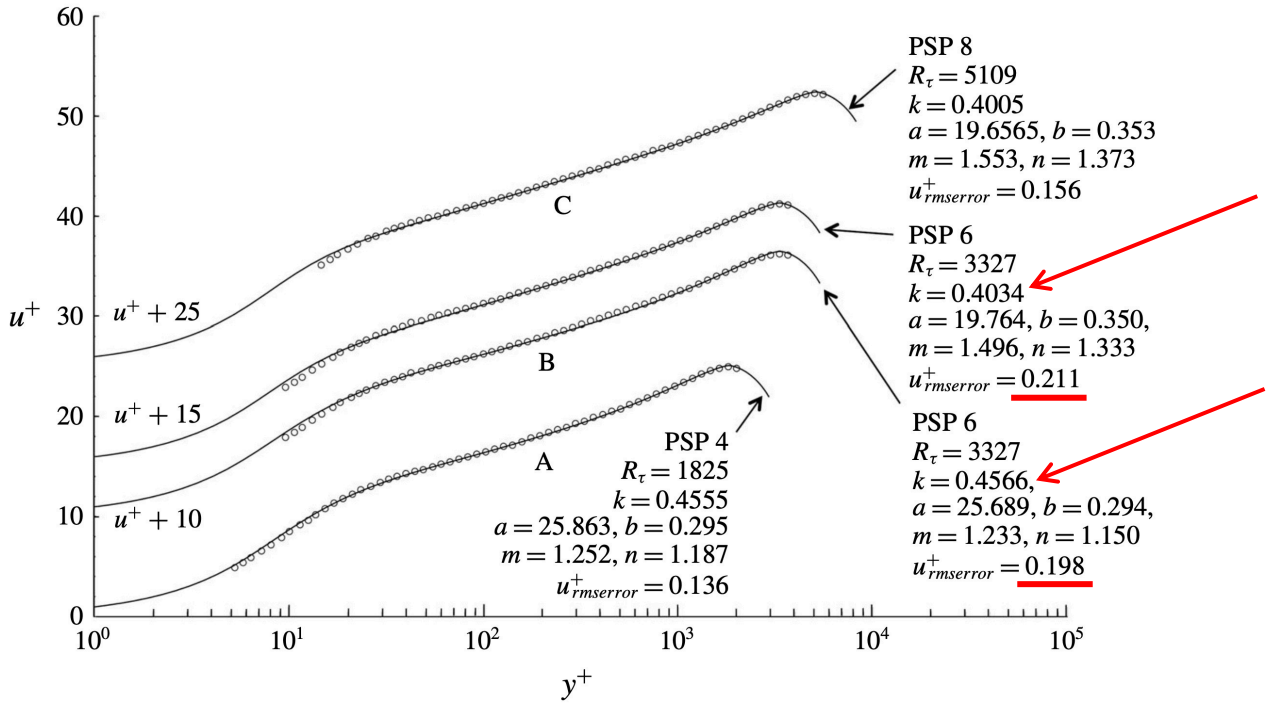

FIGURE 11. PSP 4, 6 and 8 velocity surveys are shown. The survey data (open circles ○) and comparison velocity profiles, equations (3.5) and (3.13), with optimal values of (k, a, m, b, n) are displaced 10, 15 and 25 units in u^+. PSP 6 is shown with two approximate profiles defined by two relatively different sets of optimal parameters. Each set of (k, a, m, b, n) values define a local minimum in $u^+_{rmserror}$ identified by the procedure described in § 5. Labels A, B and C identify the intermediate region of the profile generally associated with logarithmic behaviour.

STANFORD
AERONAUTICS &
ASTRONAUTICS

Optimal values of ka, b, m and n

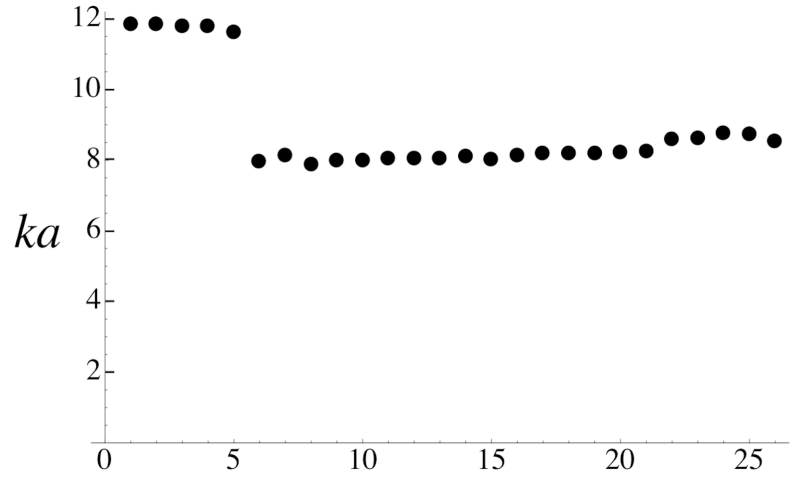

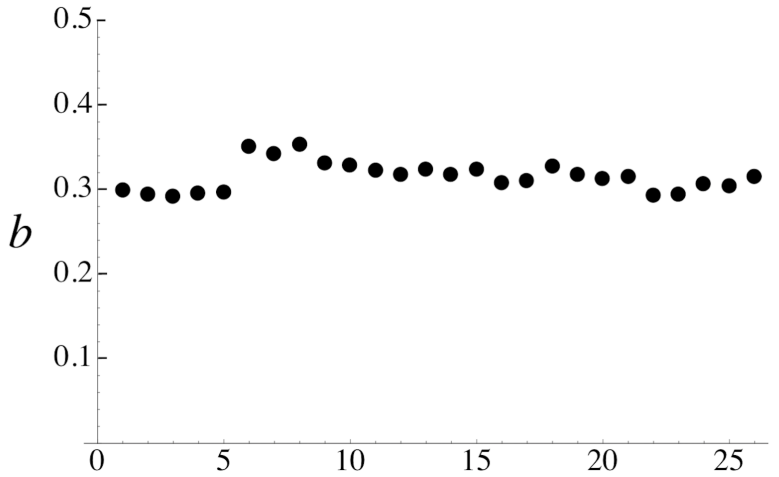

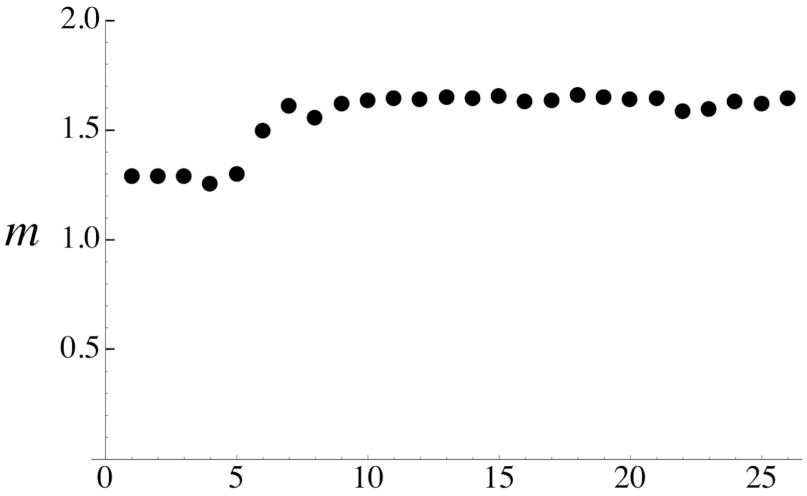

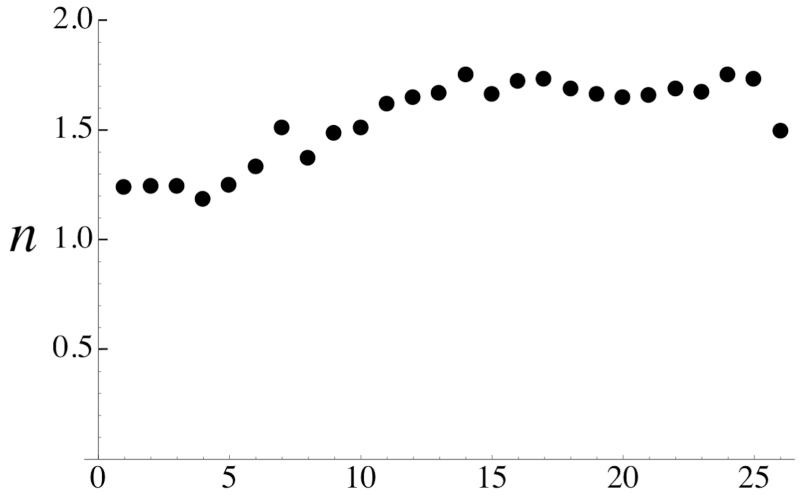

STANFORD
AERONAUTICS &
ASTRONAUTICS

Comparison between PSP data and the universal velocity profile

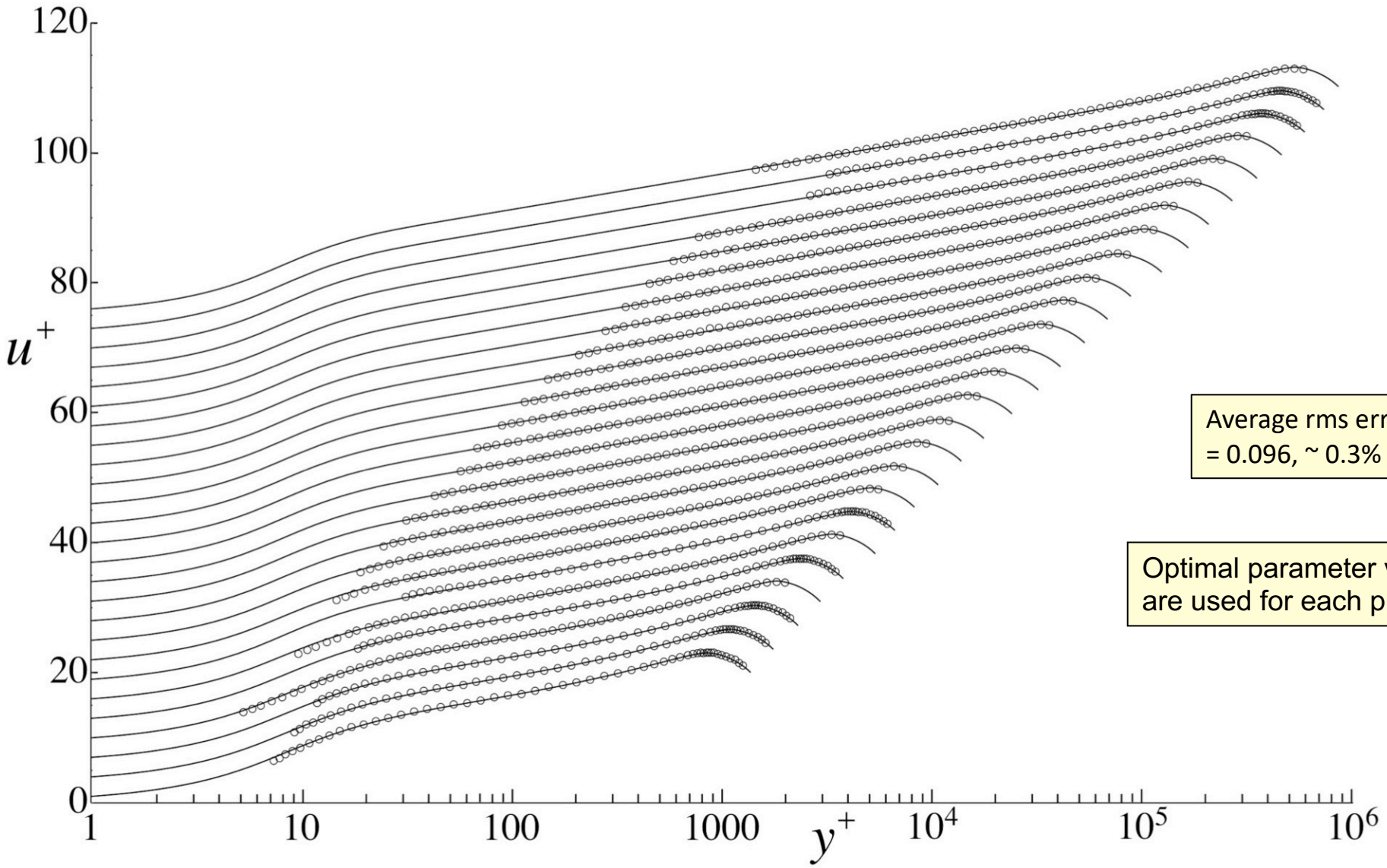

Average rms error
= 0.096, ~ 0.3%

Optimal parameter values
are used for each profile.

STANFORD
AERONAUTICS &
ASTRONAUTICS

Error

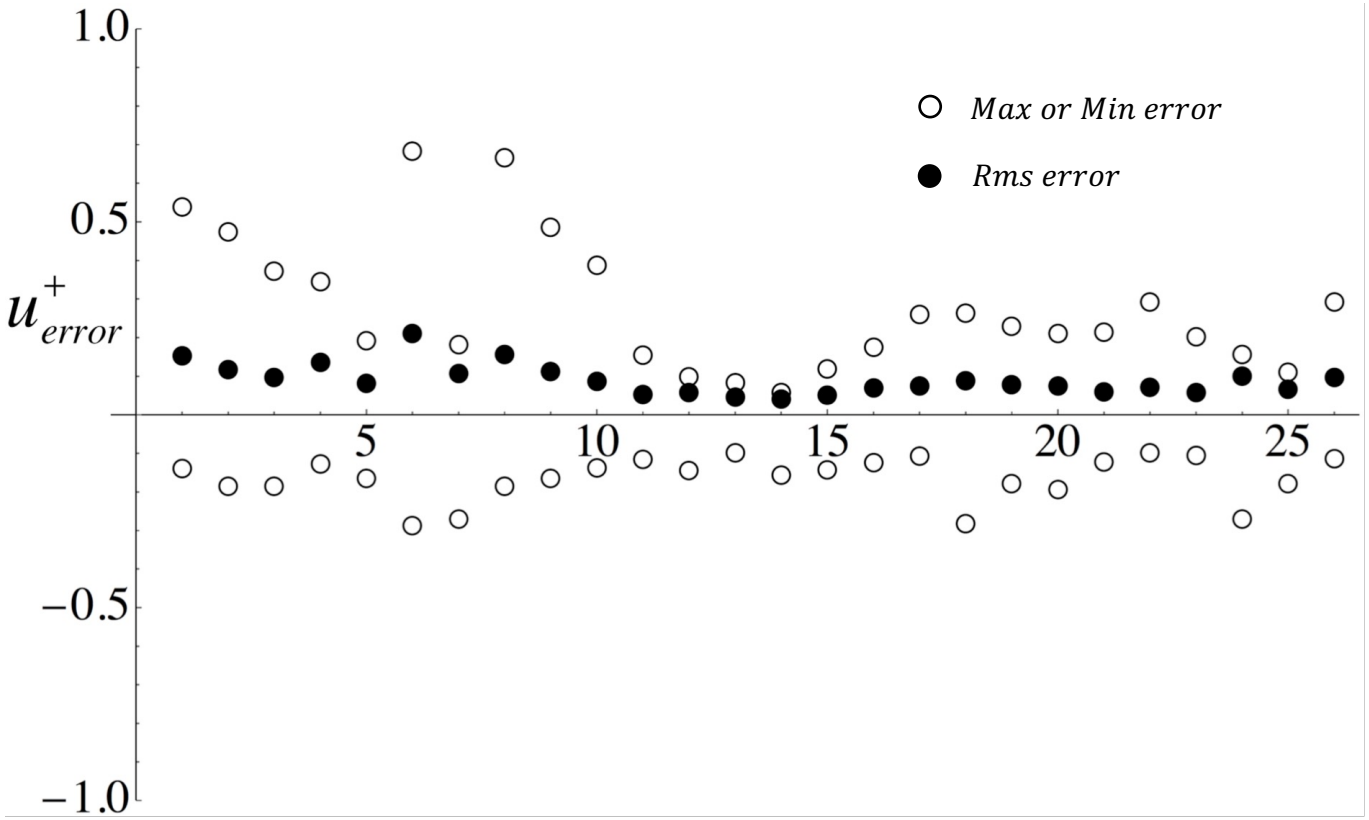

Average rms error
= 0.096, ~ 0.3%

STANFORD
AERONAUTICS &
ASTRONAUTICS

PSP Survey 23

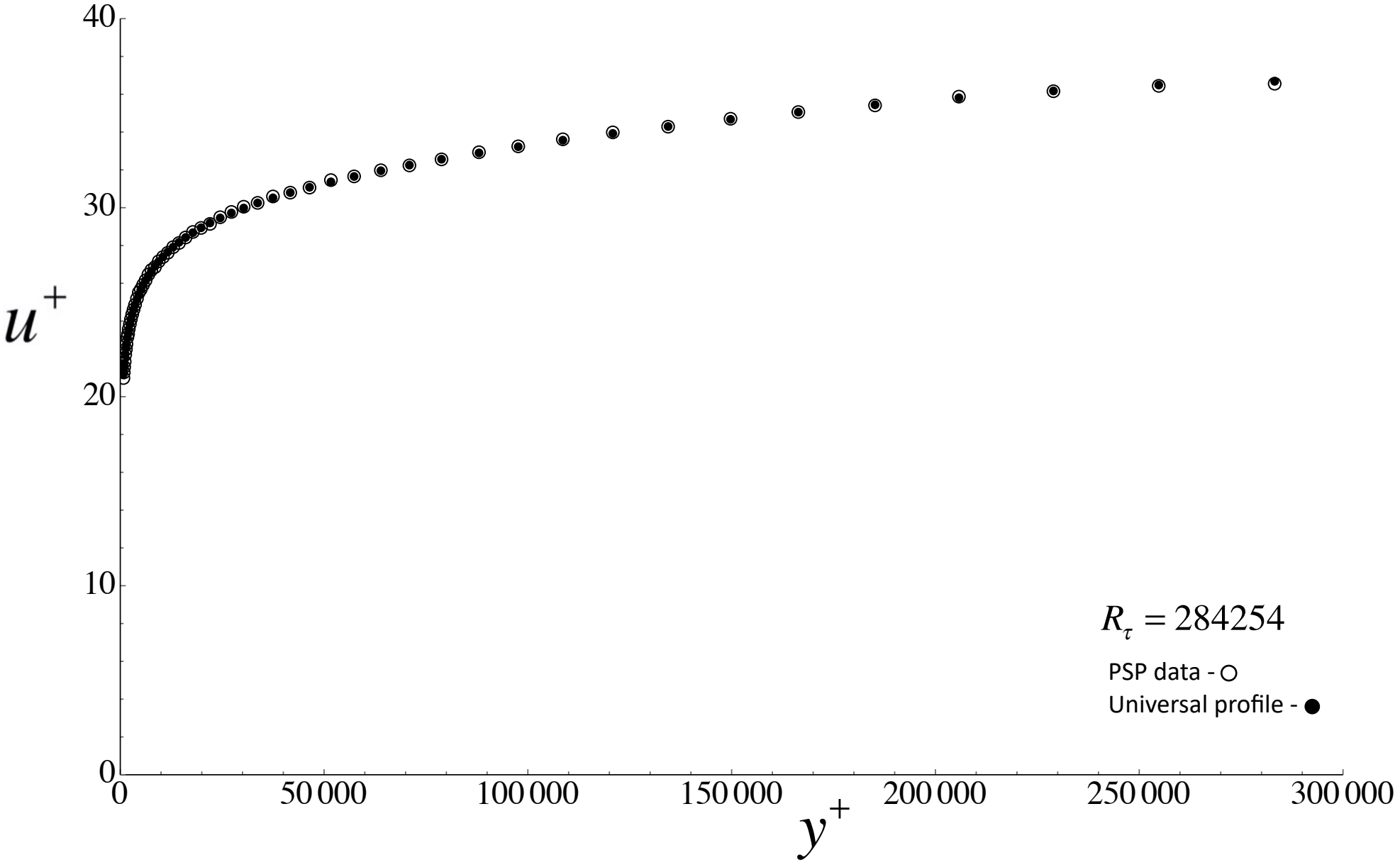

STANFORD
AERONAUTICS &
ASTRONAUTICS

PSP Smooth-wall Pipe Flow, $R_\tau = 851\ to\ 530023$

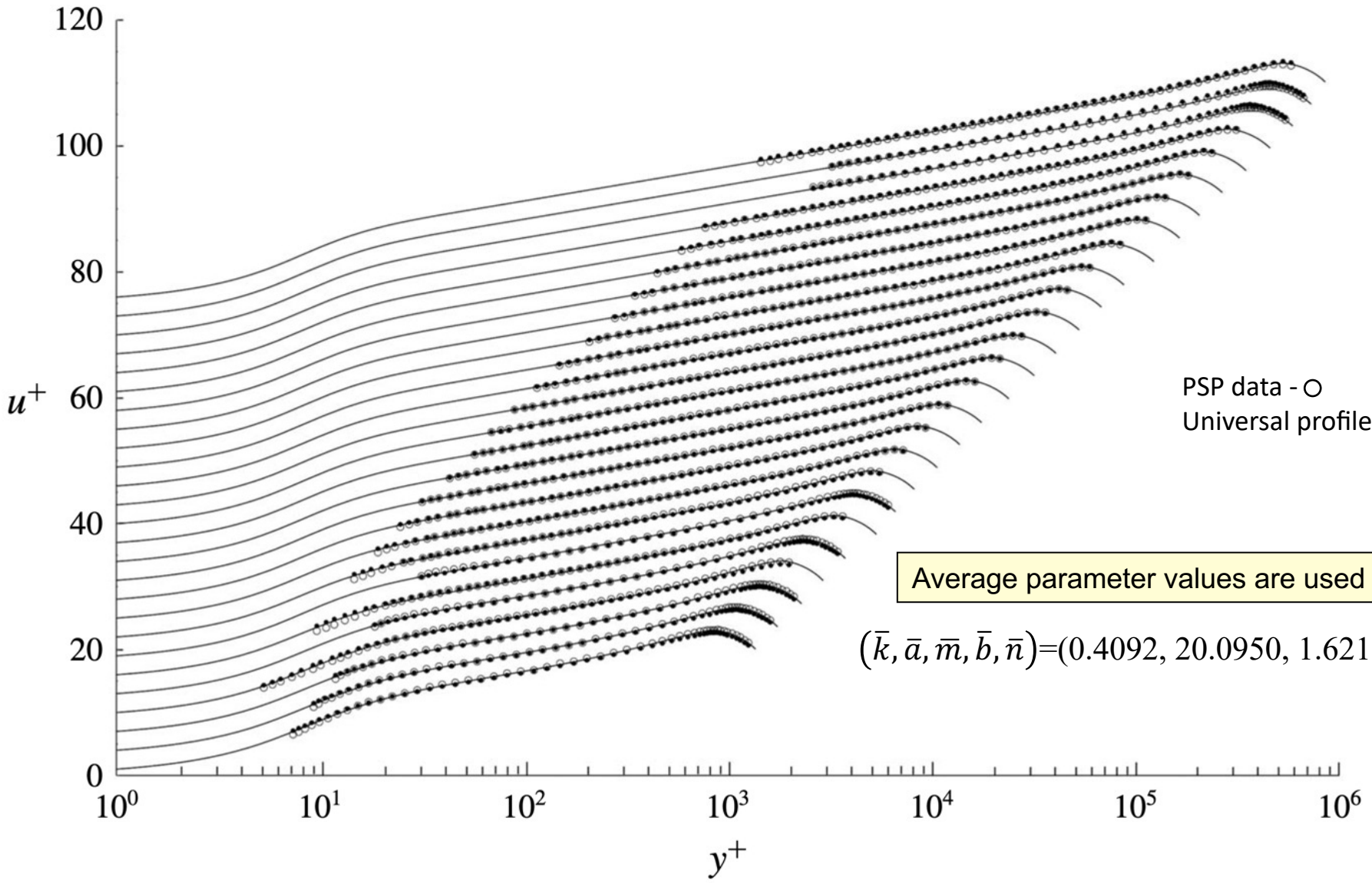

PSP data - ○
Universal profile - ●

Average parameter values are used for each profile.

$(\bar{k}, \bar{a}, \bar{m}, \bar{b}, \bar{n})$=(0.4092, 20.0950, 1.6210, 0.3195, 1.6190)

STANFORD
AERONAUTICS &
ASTRONAUTICS

PSP friction law

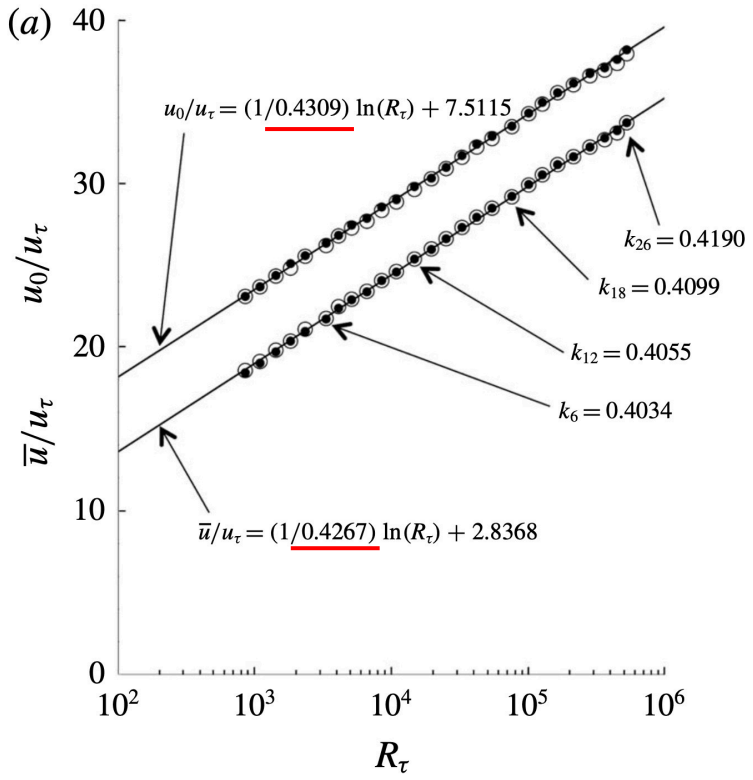

The open circles are the PSP data from each of 26 profiles. The filled circles are determined from the UVP with optimal values of (k,a,m,b,n) for each point. Optimal values of k for several PSP profiles are also shown in the figure. Note that the value of k given in the friction law is larger than any of the k values from the individual profiles.

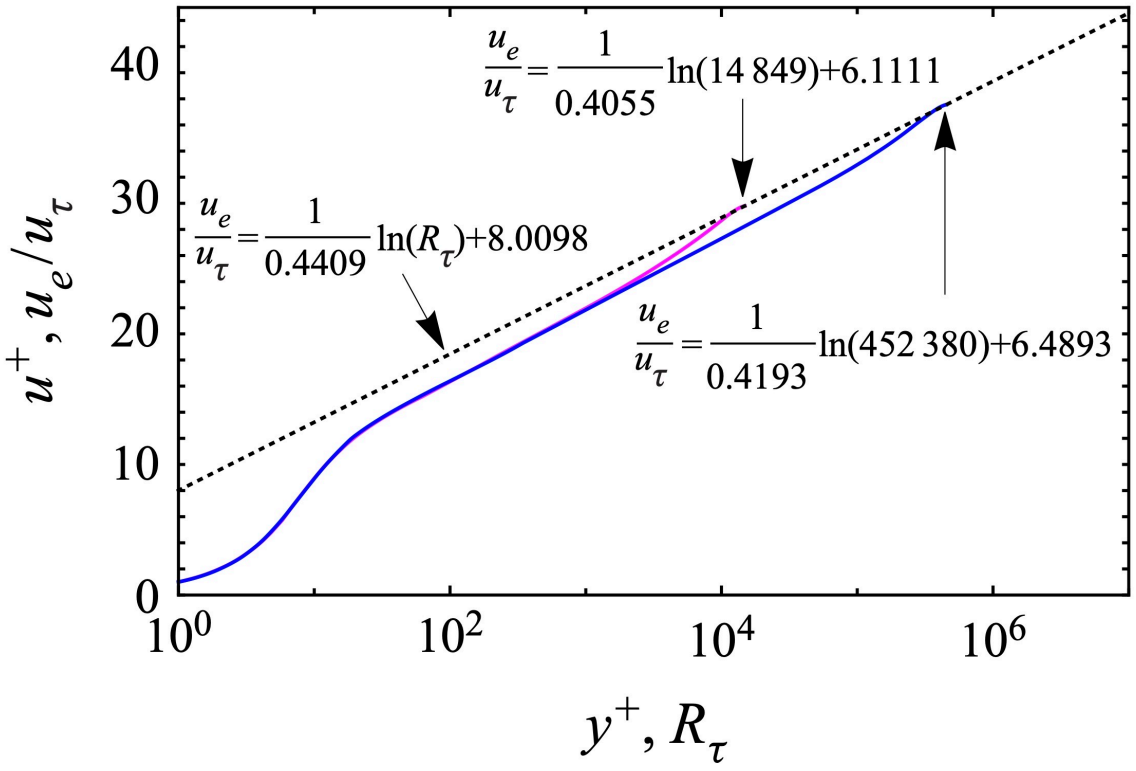

Here is the explanation. Two PSP velocity profiles at R_τ = 14849 (magenta) and R_τ = 452380 (blue). The values of k and C for each profile are indicated and the arrows point to u_e/u_τ for each profile. The dashed line is the friction law generated when the two end points are joined by a straight line.

Channel Flow

STANFORD
AERONAUTICS & ASTRONAUTICS

Channel Flow, $R_\tau = 550$ *to* 8016

Average rms error
= 0.044, ~ 0.18%

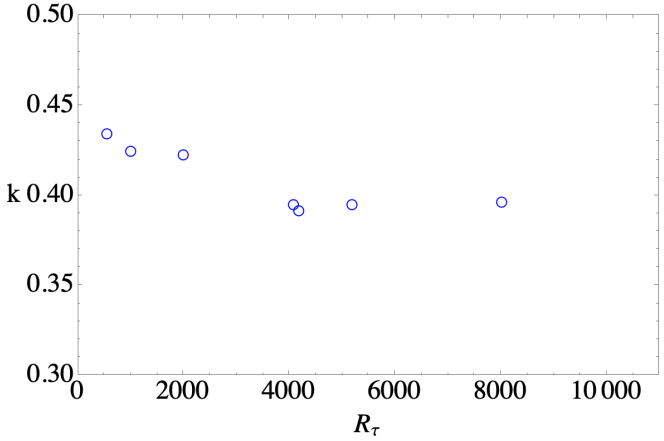

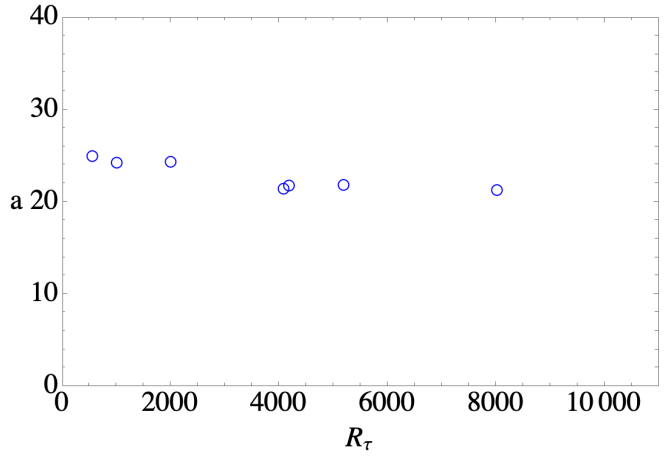

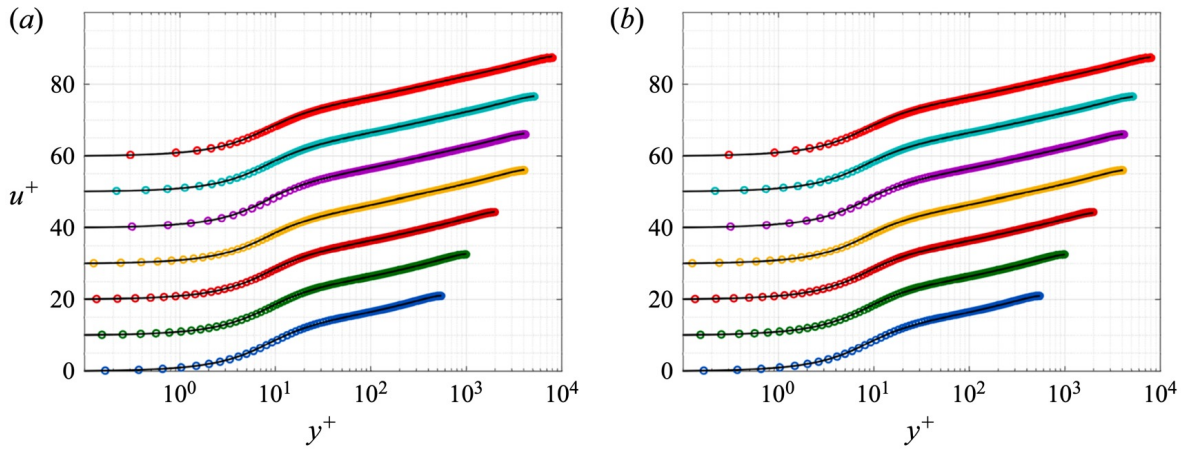

Figure 6. Channel flow velocity profiles from Lee & Moser (2015), Lozano-Durán & Jiménez (2014), Bernardini *et al.* (2014) and Yamamoto & Tsuji (2018) overlaid on the universal velocity profile with (*a*) optimal parameters from table 3 and (*b*) average parameter values from table 1 for $(\bar{k}, \bar{a}, \bar{m}, \bar{b}, \bar{n})$ at $R_\tau = 550$ (dark blue), 1001 (green), 1995 (dark red), 4079 (yellow), 4179 (purple), 5186 (light blue), 8016 (light red). Profiles are separated vertically by 10 units.

R_τ	$(u_e/u_\tau)_{data}$	$(u_e/u_\tau)_{uvp}$	k	a	m	b	n	u^+_{rms}
550	21.0008	21.0595	0.4344	24.9898	1.2504	0.4237	1.3395	0.055682
1001	22.5932	22.6511	0.4247	24.2801	1.2341	0.4289	1.3058	0.051927
1995	24.3959	24.4841	0.4227	24.3731	1.2164	0.4307	1.2588	0.043820
4079	25.9546	26.0605	0.3950	21.4550	1.2607	0.4654	1.4602	0.042982
4179	25.9565	26.1392	0.3916	21.7990	1.3035	0.5020	1.5284	0.038933
5186	26.5753	26.6803	0.3950	21.8670	1.2667	0.4472	1.5700	0.043438
8016	27.3808	27.5914	0.3964	21.3074	~~1.2828~~ 1.199	0.5558	1.3171	0.032911

Table 3. Reynolds number, optimal model parameters and root-mean-square (r.m.s.) error for channel flow datasets. Second column is extrapolation of u/u_τ data to channel centreline. Third column is u_e/u_τ calculated using the universal velocity profile (*uvp*).

Average parameter values are used for each profile on the right.

$$(\bar{k}, \bar{a}, \bar{m}, \bar{b}, \bar{n}) = (0.4086,\ 22.8673,\ 1.2569,\ 0.4649,\ 1.3972)$$

Zero Pressure Gradient Turbulent Boundary Layer

STANFORD
AERONAUTICS &
ASTRONAUTICS

ZPG Turbulent Boundary Layer experimental data, $R_\tau = 2109\ to\ 17207$

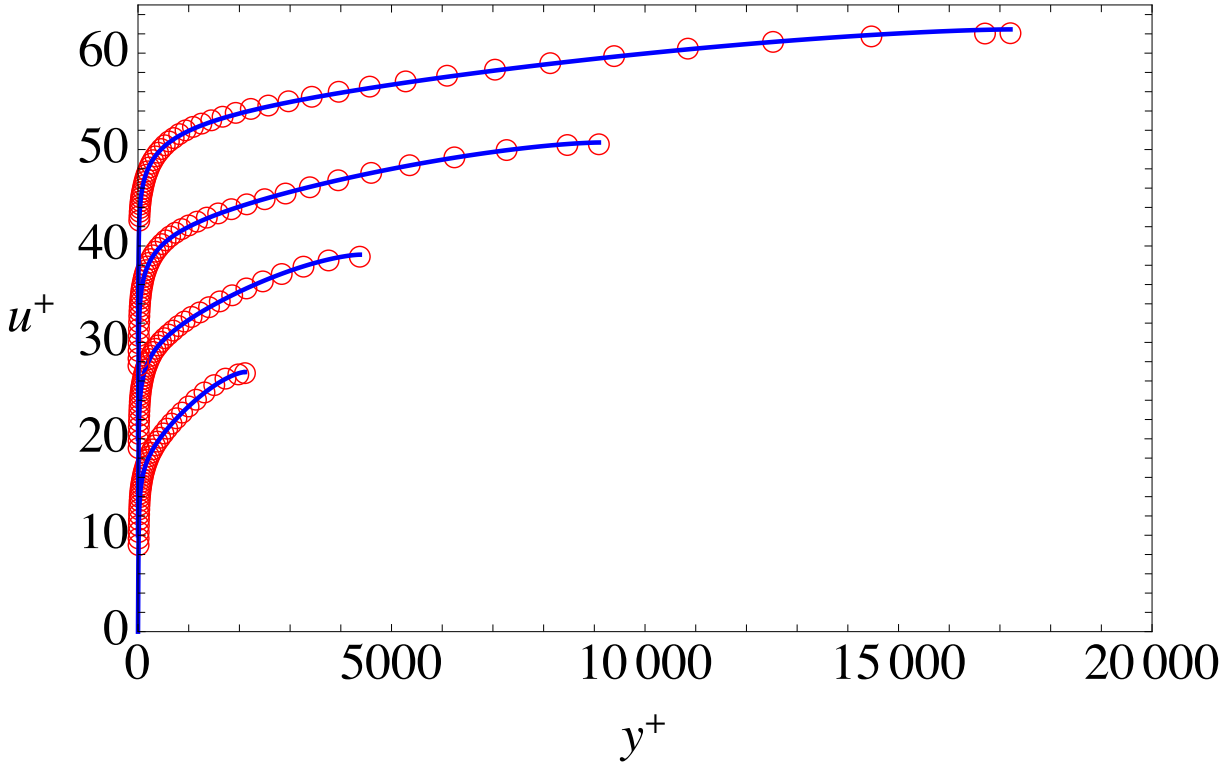

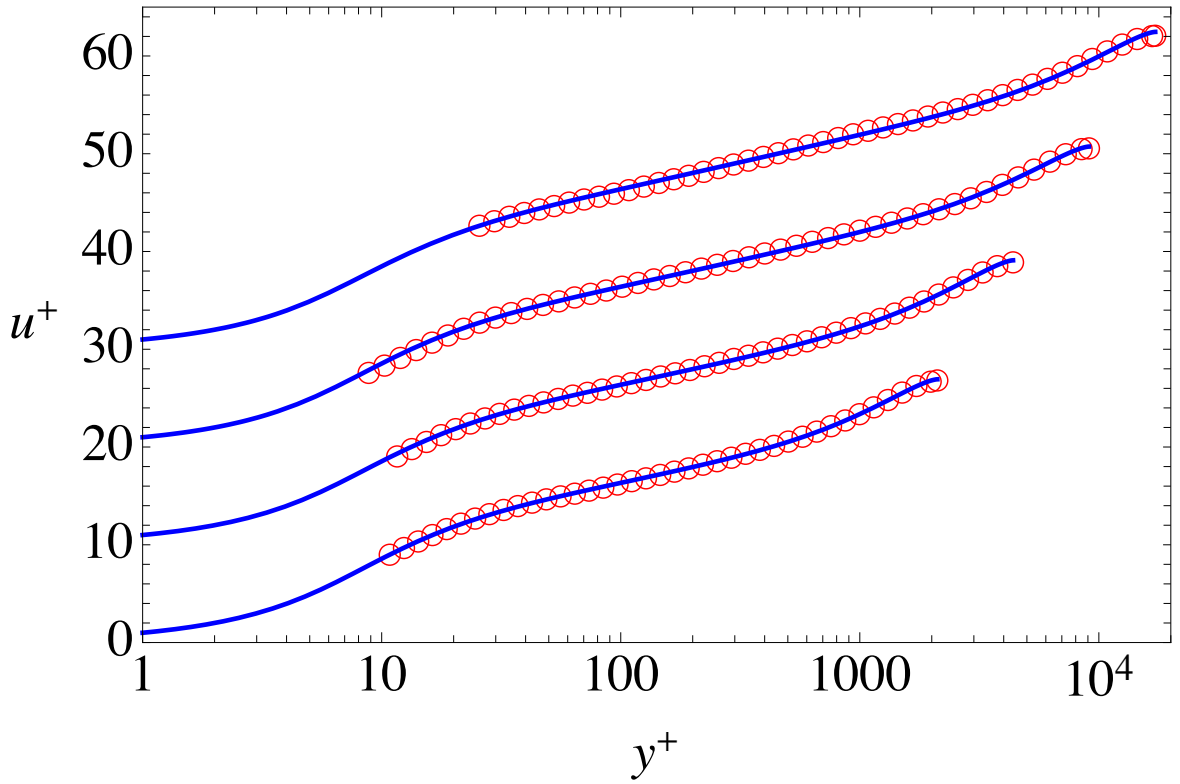

R. Baidya, J. Phillip, N. Hutchins, J.P. Monty & I. Marusic 2021 Spanwise velocity statistics in high-Reynolds-number turbulent boundary layers. *J. Fluid Mech.* 913, A35.

ZPG TBL computational data, $R_\tau = 1343\ to\ 2571$

Average rms error
= 0.033, ~ 0.13%
$\delta_h = \delta_{0.993} - \delta_{0.996}$

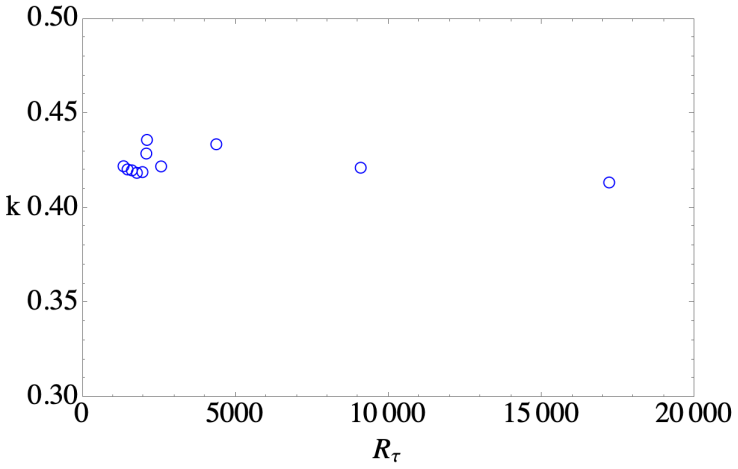

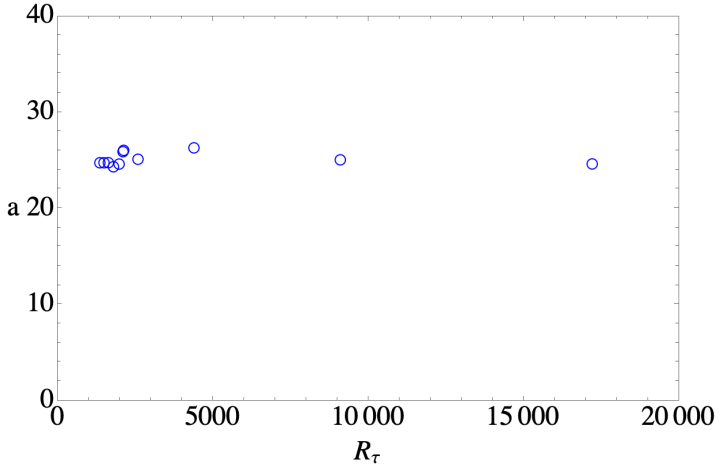

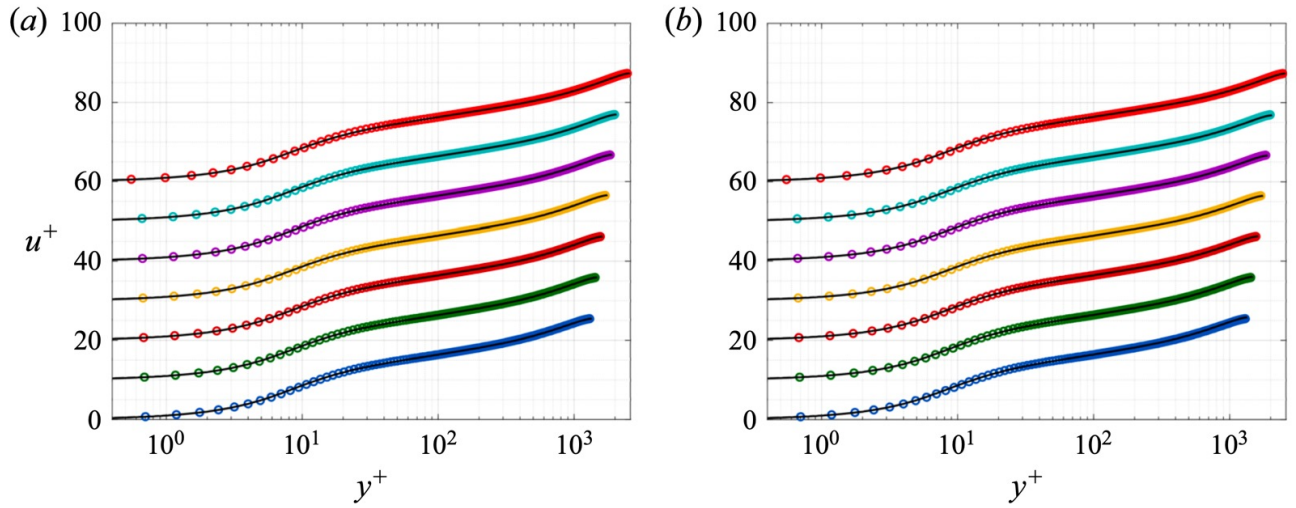

Figure 12. Turbulent boundary layer DNS data from Simens *et al.* (2009), Borrell *et al.* (2013), Sillero *et al.* (2013) and Eitel-Amor *et al.* (2014) at $R_\tau = 1343$ (dark blue), 1475 (green), 1616 (dark red), 1779 (yellow), 1962 (purple), 2088 (light blue) and 2571 (light red) compared with the universal velocity profile using (*a*) optimal parameters from table 4, (*b*) average parameters from 1. Profiles are separated vertically by 10 units.

Average parameter values are used for each profile on the right.

$(\bar{k}, \bar{a}, \bar{m}, \bar{b}, \bar{n})$=(0.4233, 24.9583, 1.1473, 0.1752, 2.1707)

R_τ	$(u_e/u_\tau)_{data}$	$(u_e/u_\tau)_{uvp}$	k	a	m	b	n	u^+_{rms}	u_e/U
1343	25.5088	25.4939	0.4222	24.7756	1.1820	0.1828	2.3298	0.03617	0.993
1475	25.9305	25.8994	0.4205	24.7786	1.1732	0.1787	2.3622	0.03332	0.993
1616	26.2722	26.2365	0.4200	24.7834	1.1720	0.1764	2.3548	0.03390	0.993
1779	26.5926	26.5818	0.4187	24.3610	1.2032	0.1757	2.2932	0.03215	0.994
1962	26.8226	26.8512	0.4191	24.6388	1.1752	0.1747	2.2833	0.03298	0.994
2088	27.0332	27.0255	0.4289	25.9290	1.1480	0.1696	2.2516	0.03143	0.994
2571	27.4177	27.4073	0.4221	25.1424	1.1130	0.1724	2.3087	0.03150	0.993
2109	26.8104	26.9239	0.4361	26.0709	1.1410	0.1665	2.1993	0.05453	0.996
4374	28.8876	29.0940	0.4338	26.3286	1.1060	0.1664	1.8792	0.09473	0.996
9090	30.5483	30.7301	0.4214	25.0804	1.1216	0.1829	1.7753	0.13364	0.996
17 207	32.0670	32.4649	0.4136	24.6549	1.0846	0.1816	1.8397	0.16864	0.996

Turbulent Boundary Layer equivalent channel half height (overall thickness) δ_h

δ_h is defined as the thickness that minimizes the error between a specific data set and the UVP

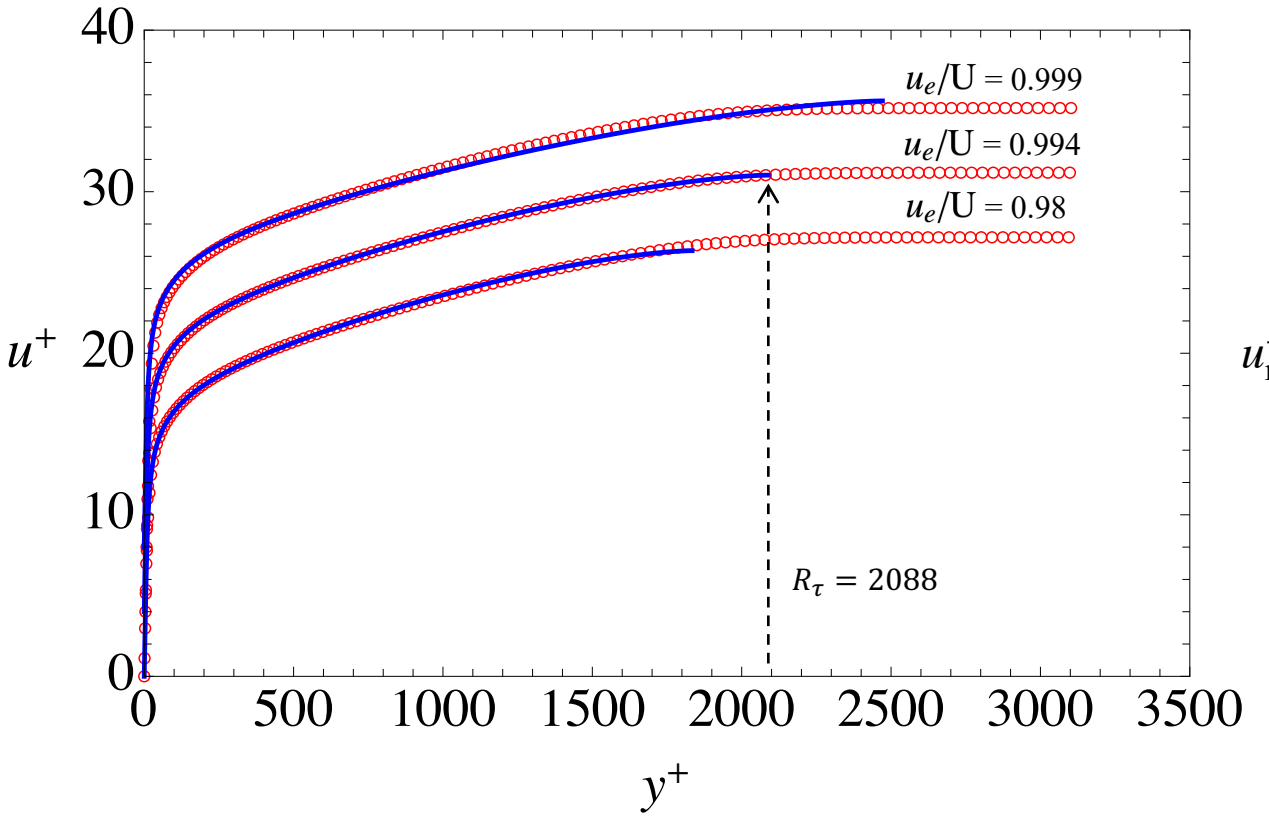

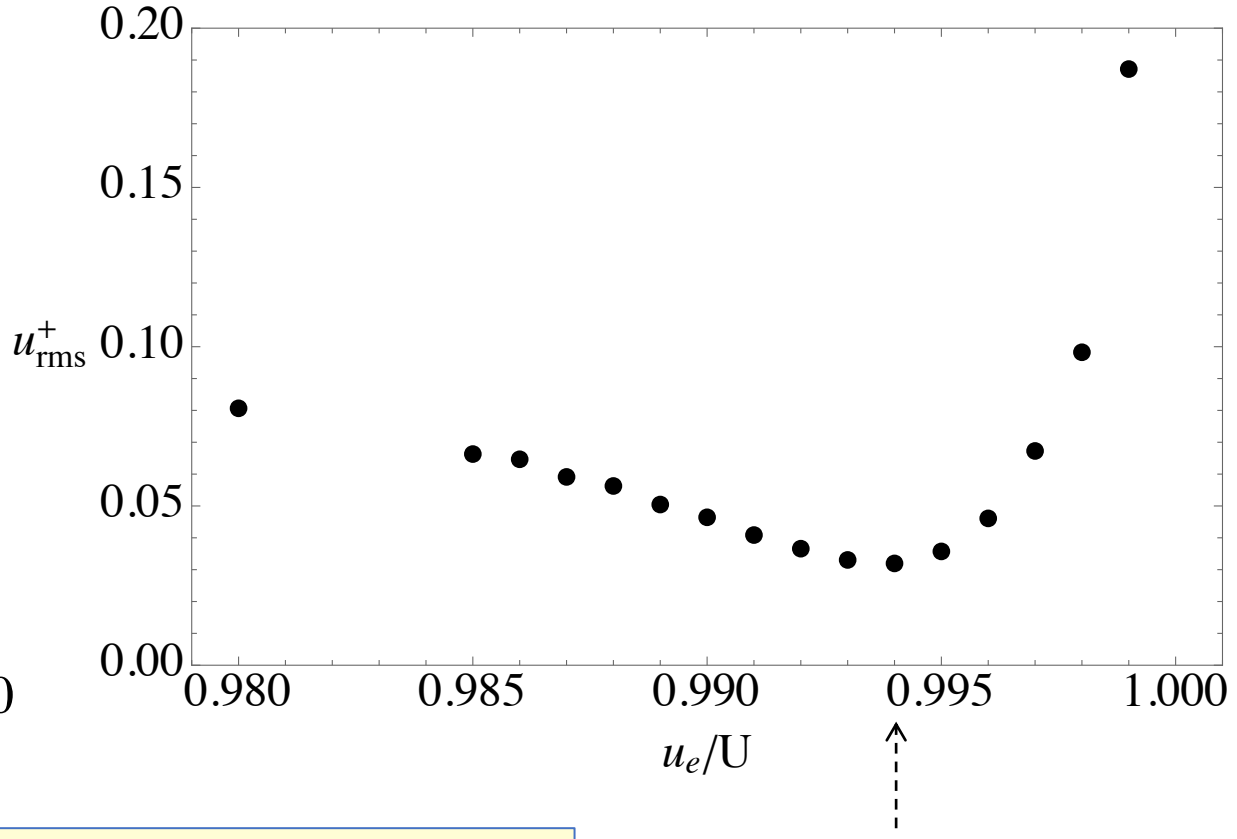

DNS data is from

J. A. Sillero, J. Jimenez & R. D. Moser 2013 One-point statistics for turbulent wall-bounded flows at Reynolds numbers up to δ+ = 2000. *Phys. Fluids* 25 (10), 105102.

Average parameter values for pipe, channel and ZPG boundary layer flows

TABLE I. Average model parameters with standard deviation for basic wall flows. Ranges of R_τ for each flow are as follows: Pipe (3327–530 023), Channel (550–8016), ZPG boundary layer (1343–17 207).

Flow	$\bar{k}$	σ_k	$\bar{a}$	σ_a	$\bar{m}$	σ_m	$\bar{b}$	σ_b	$\bar{n}$	σ_n
Pipe (21 profiles)	0.4092	0.0057	20.0950	0.381	1.6210	0.0379	0.3195	0.0157	1.6190	0.1204
Channel (7 profiles)	0.4086	0.0179	22.8673	1.599	1.2569	0.0292	0.4649	0.0485	1.3972	0.1213
ZPG boundary layer (11 profiles)	0.4233	0.0068	24.9583	0.663	1.1473	0.0373	0.1752	0.0060	2.1707	0.2238

The UVP boundary layer friction law (blue line)

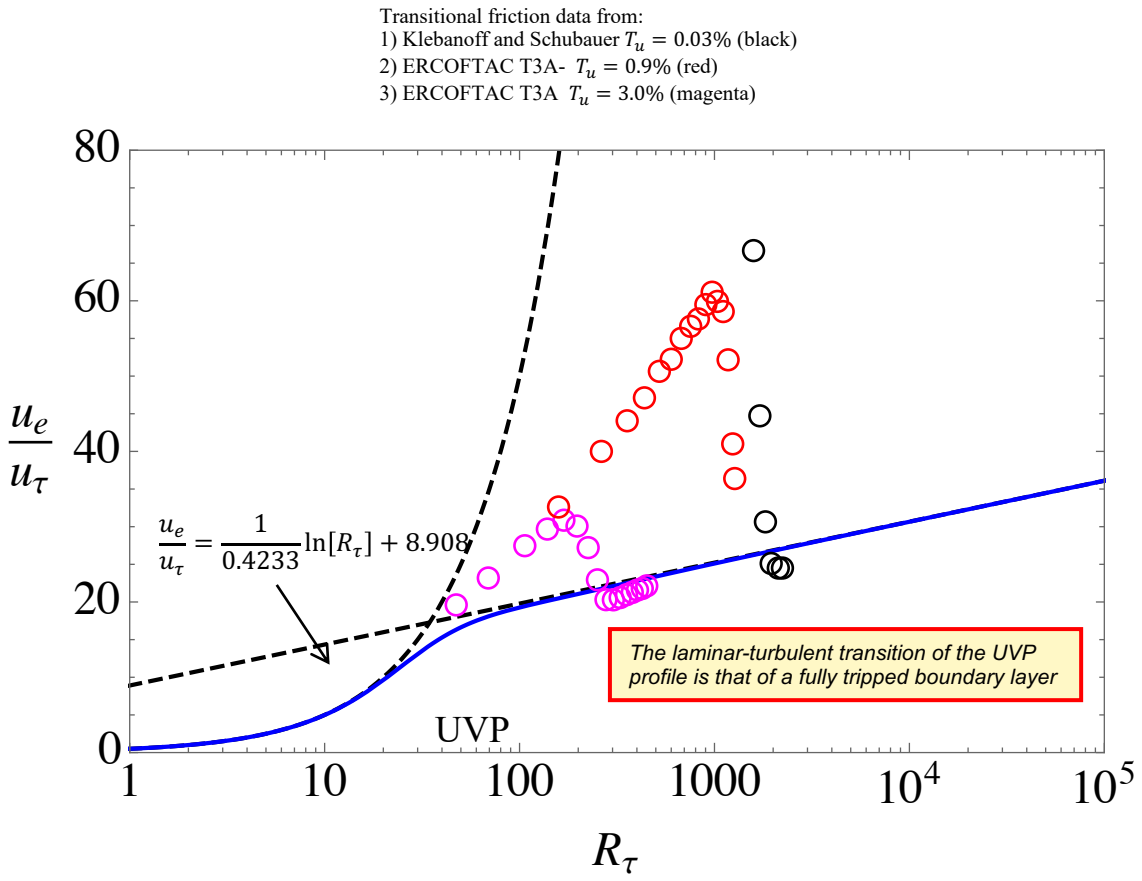

FIG. 9. The universal velocity profile friction law for a zero pressure gradient boundary layer along with transitional friction data from Schubauer and Klebanoff[30] (natural transition $T_u = 0.03\%$—black) and Coupland[31] (ERCOFTAC case T3A $T_u = 0.9\%$—red, case T3A $T_u = 3.0\%$—magenta).

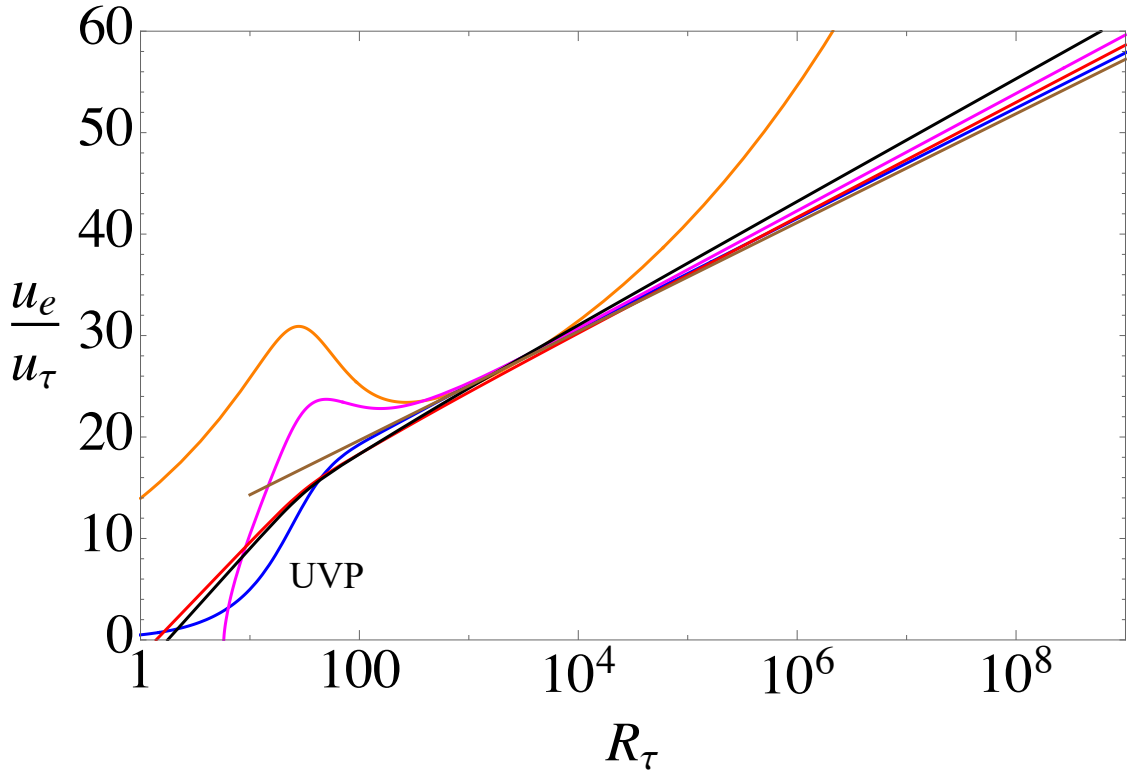

FIG. 10. Five friction laws compared to the UVP (blue line). The orange line is the Ludwieg–Tillman law[6] used in Head's method. The magenta line is the friction law developed by Nash.[34] The red and black lines are two versions of the Coles–Fernholz law with $(k, C) = (0.41, 5.0)$ (red line) and $(k, C) = (0.384, 4.1)$ (black line). The brown line is the Spalart–Allmaras law, Eq. (34), deduced from data in Polewski and Cizmas.[36]

Turbulent Boundary Layer Flow with Pressure Gradient

STANFORD
AERONAUTICS &
ASTRONAUTICS

Adverse pressure gradient Turbulent Boundary Layer experimental data, $R_\tau = 2461\ to\ 3587$

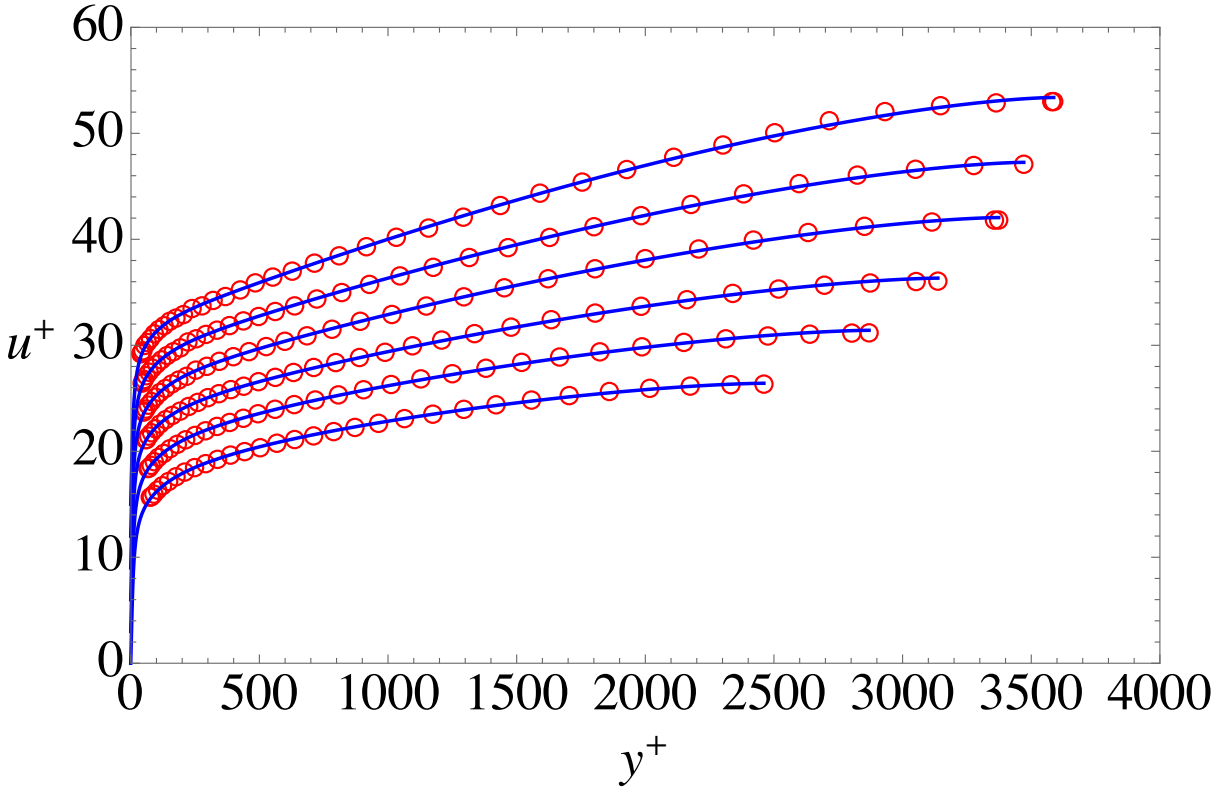

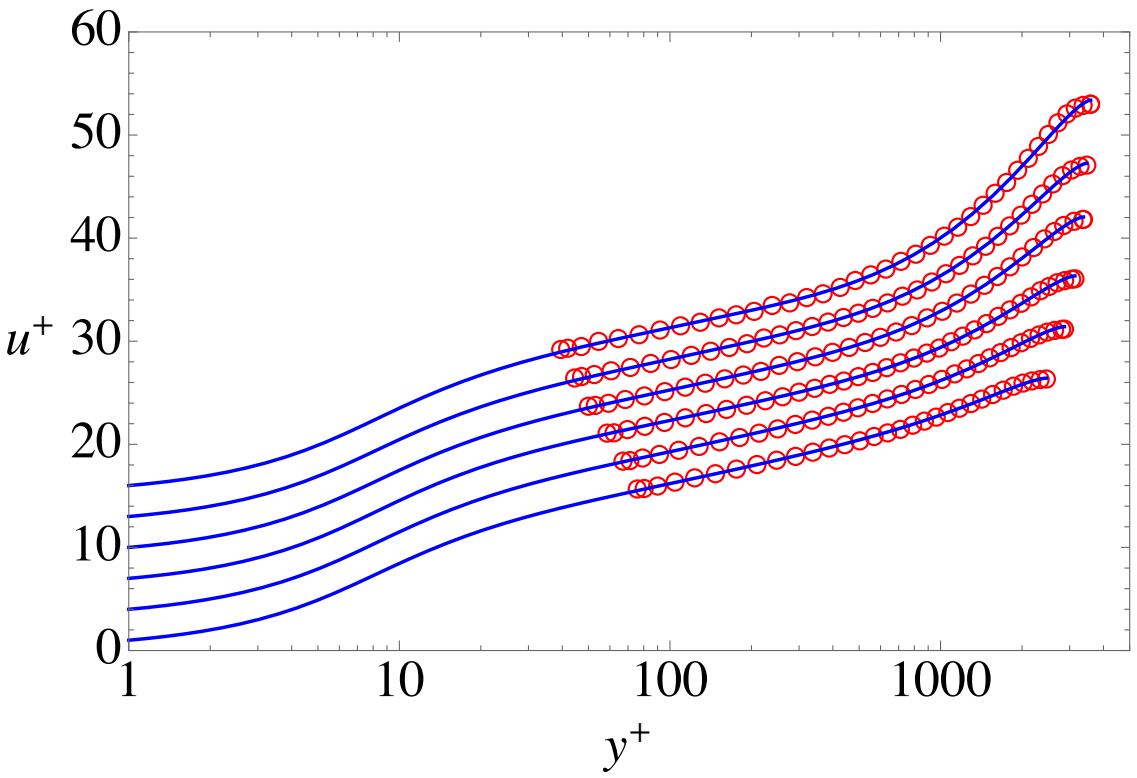

Perry, A.E. & Marusic, I. 1995 A wall-wake model for the turbulence structure of boundary layers. Part 1. Extension of the attached eddy hypothesis. *J. Fluid Mech.* 298, 361–388.

Average rms error = 0.148, ~ 0.46% δ_h=$\delta_{0.998}$

STANFORD AERONAUTICS & ASTRONAUTICS

Changes in boundary layer wall parameters (k, a, m) in an adverse pressure gradient are small.

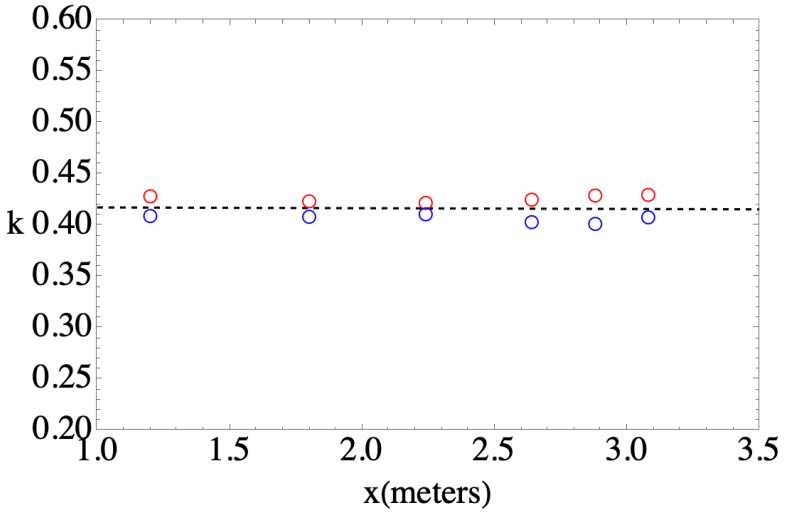

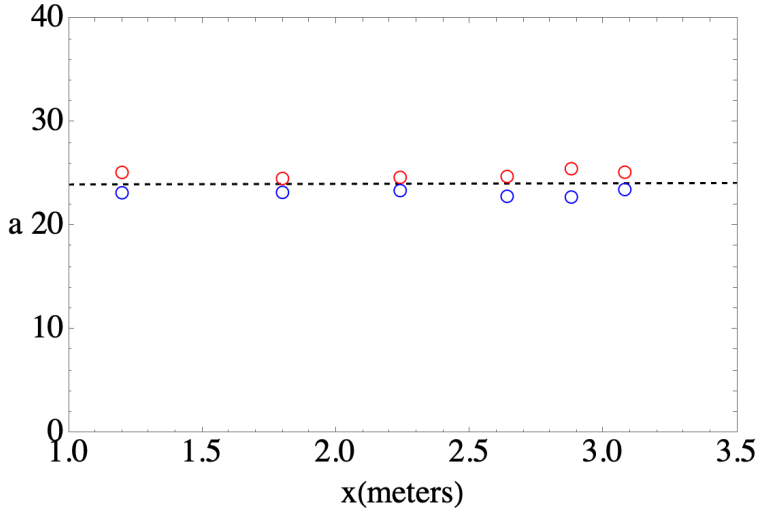

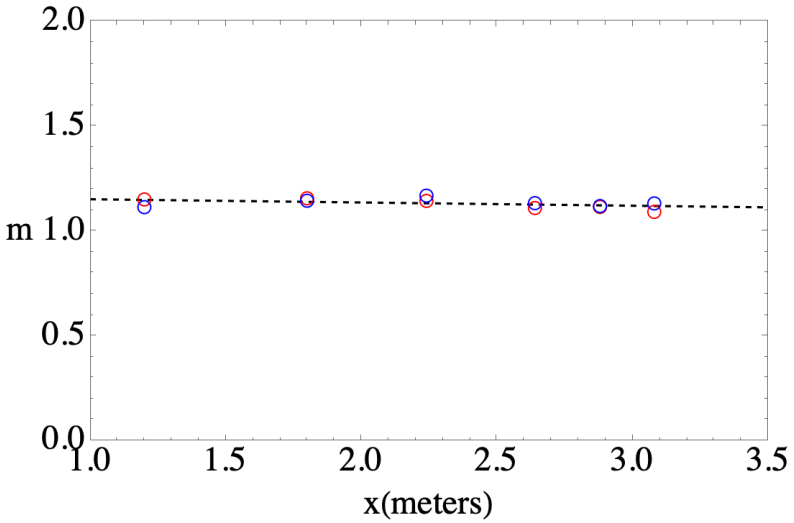

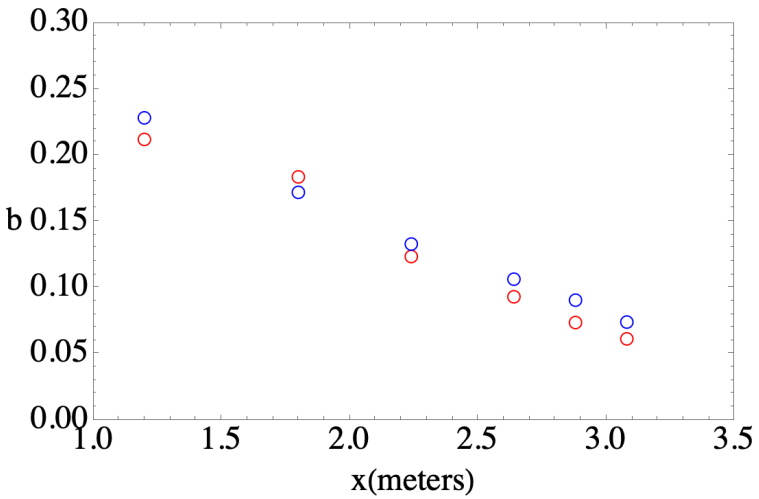

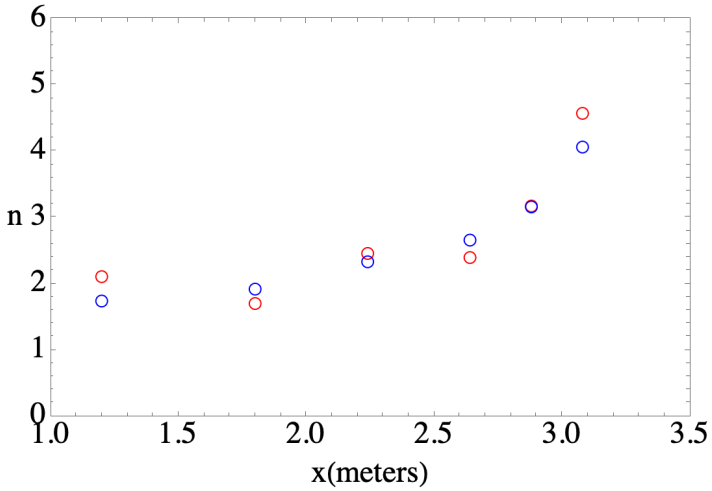

u_∞=10 m/sec

u_∞=30 m/sec

STANFORD
AERONAUTICS &
ASTRONAUTICS

Parameters for the adverse pressure gradient cases

TABLE II. Run data, Reynolds number, optimal model parameters, and RMS error for adverse pressure gradient boundary layer datasets from Perry and Marusic.[27] Initial free stream values are $u_\infty = 10$ and $u_\infty = 30$ m/s. Channel half height thickness for these data are at $u = 0.998u_e$; $\delta_h = \delta_{0.998}$. Reprinted with permission from Subrahmanyam *et al.*, J. Fluid Mech. **933**, A16 (2022). Copyright 2022 Author(s), licensed under a Creative Commons Attribution (CC BY) License.[17]

x (m)	$u_e\left(\frac{\text{m}}{\text{s}}\right)$	R_{δ_1}	R_{δ_2}	β	β_c	δ_{998} (m)	$R_{\delta_{998}}$	R_τ	$\left(\frac{u_e}{u_\tau}\right)$	k	a	m	b	n	$u^+{}_{rms}$
1.20	10.361	3 165	2 282	0.0	0.0	0.031 79	21 439	912	23.51	0.4287	25.18	1.1528	0.212 2	2.111	0.120
1.80	9.976	5 226	3 734	0.65	1.115	0.050 19	32 606	1285	25.37	0.4239	24.59	1.1583	0.183 9	1.705	0.253
2.24	9.256	6 410	4 342	1.45	2.432	0.055 43	33 456	1195	28.00	0.4223	24.70	1.1460	0.123 7	2.461	0.163
2.64	8.588	8 606	5 517	2.90	4.760	0.070 55	39 406	1252	31.47	0.4255	24.79	1.1121	0.093 31	2.399	0.152
2.88	8.155	11 235	6 879	4.48	7.223	0.086 34	46 043	1337	34.44	0.4296	25.54	1.1173	0.073 83	3.178	0.220
3.08	7.896	12 397	7 213	7.16	11.326	0.092 63	47 598	1248	38.13	0.4302	25.20	1.0938	0.061 51	4.578	0.231
1.20	30.704	8 772	6 564	0.0	0.0	0.033 53	64 807	2461	26.34	0.4095	23.21	1.1161	0.228 5	1.743	0.0705
1.80	29.054	12 401	9 073	0.71	1.230	0.044 15	80 849	2870	28.17	0.4088	23.25	1.1468	0.172 2	1.922	0.0895
2.24	27.035	16 307	11 587	1.39	2.378	0.055 26	94 275	3137	30.05	0.4112	23.42	1.1710	0.133 1	2.335	0.0942
2.64	25.150	21 634	14 736	2.74	4.606	0.069 68	110 700	3373	32.82	0.4035	22.87	1.1352	0.106 6	2.663	0.0984
2.88	23.885	25 854	17 020	3.96	6.567	0.080 54	121 760	3471	35.08	0.4018	22.80	1.1213	0.090 7	3.164	0.1183
3.08	22.908	31 767	20 052	6.07	9.901	0.093 73	136 290	3587	37.99	0.4083	23.53	1.1339	0.074 2	4.069	0.1673

STANFORD
AERONAUTICS &
ASTRONAUTICS

Favorable pressure gradient Turbulent Boundary Layer experimental data, $R_\tau = 429\ to\ 1746$.

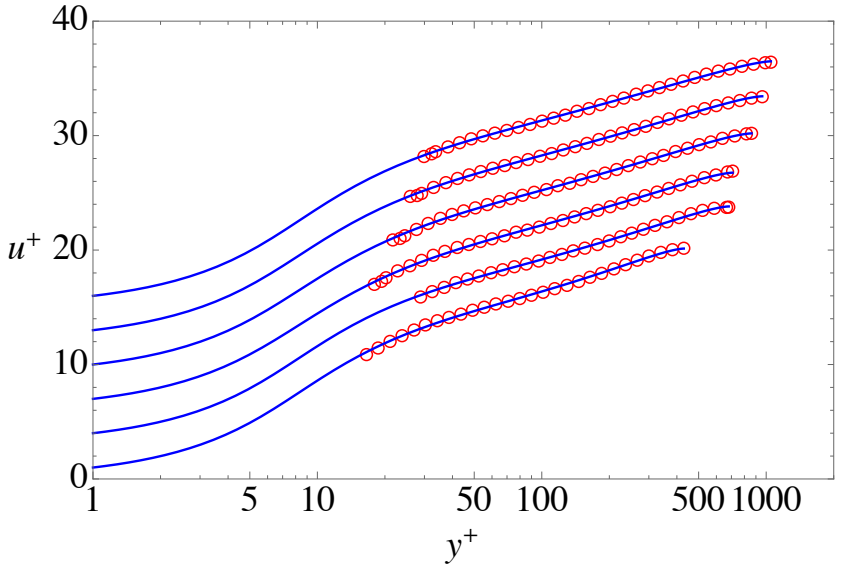

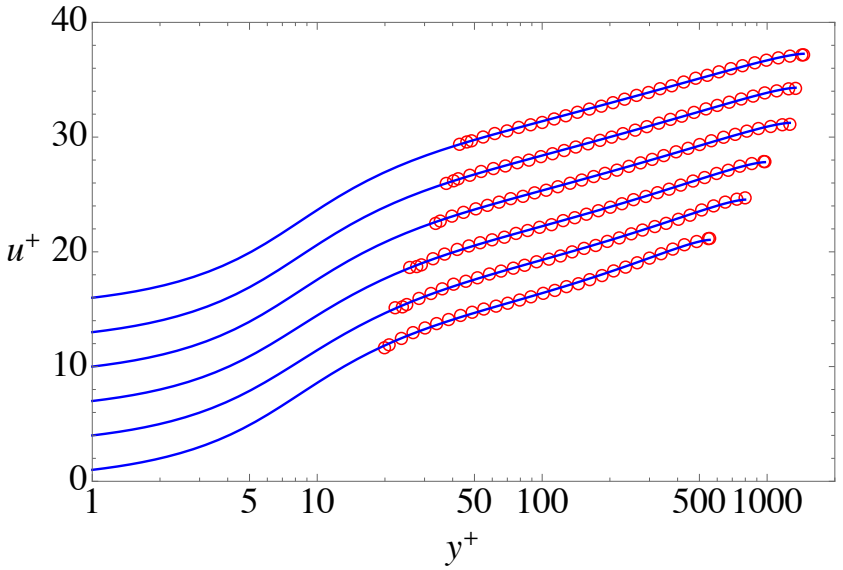

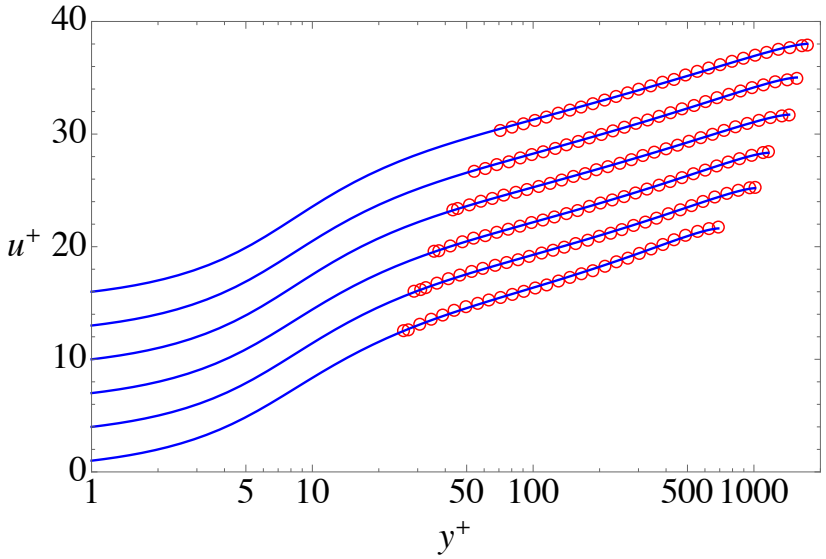

M. Jones, I. Marusic, and A. E. Perry, "Evolution and structure of sink-flow turbulent boundary layers," Journal of Fluid Mechanics 428, 1 – 27 (2001).

Average rms error = 0.075, ~ 0.36%
δ_h=$\delta_{0.996}$

STANFORD
AERONAUTICS & ASTRONAUTICS

Changes in boundary layer wall parameters (k, a, m) in a favorable pressure gradient are modest.

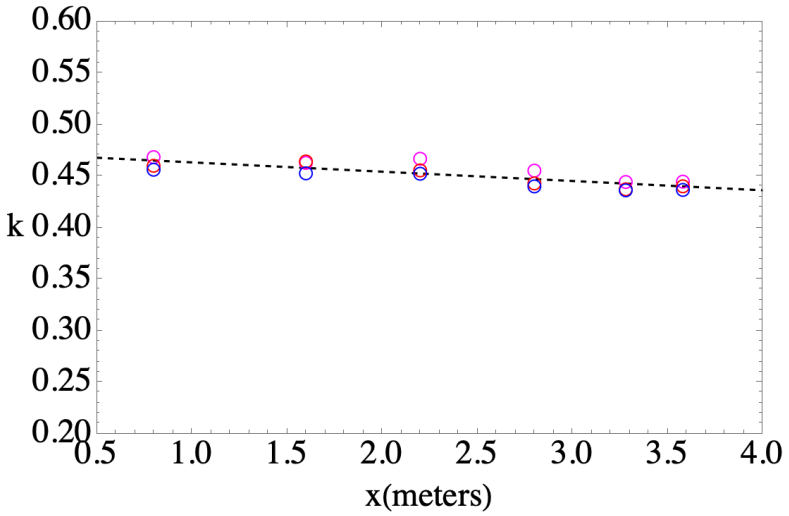

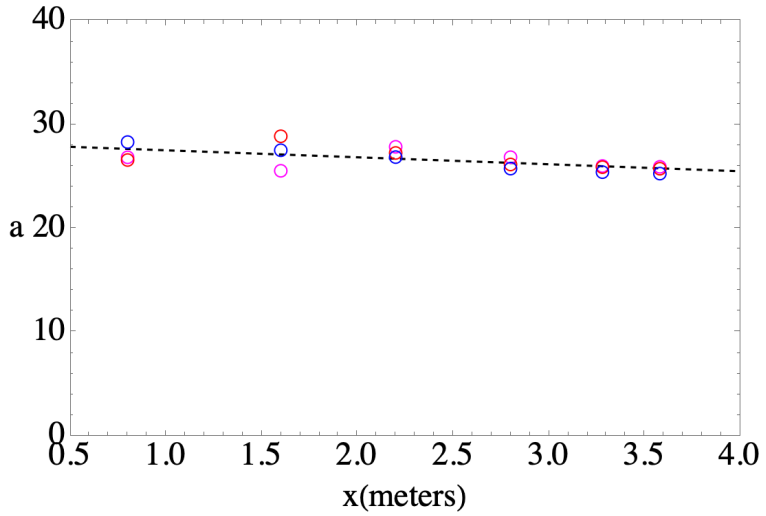

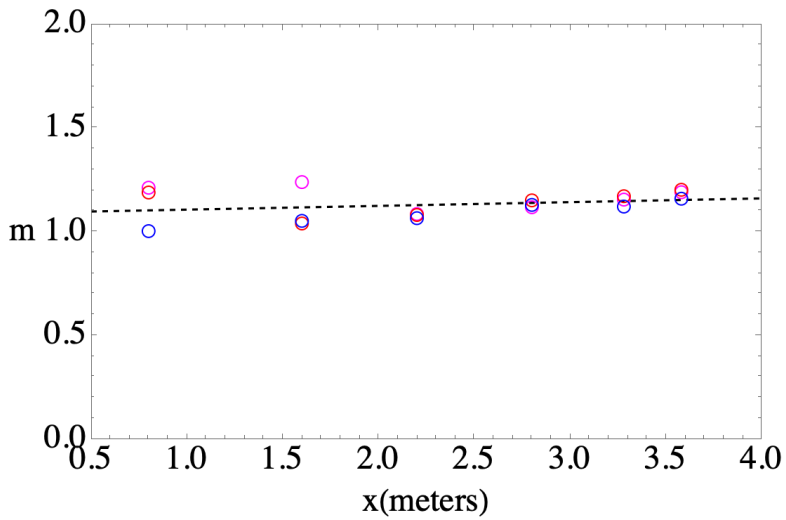

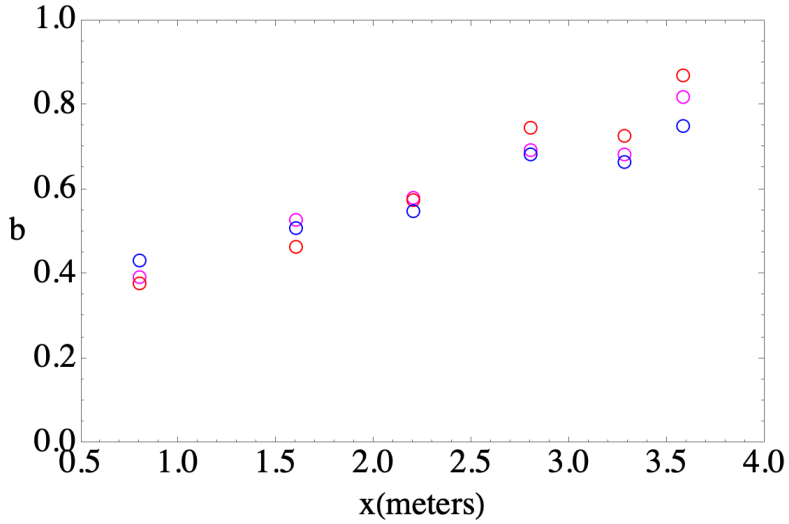

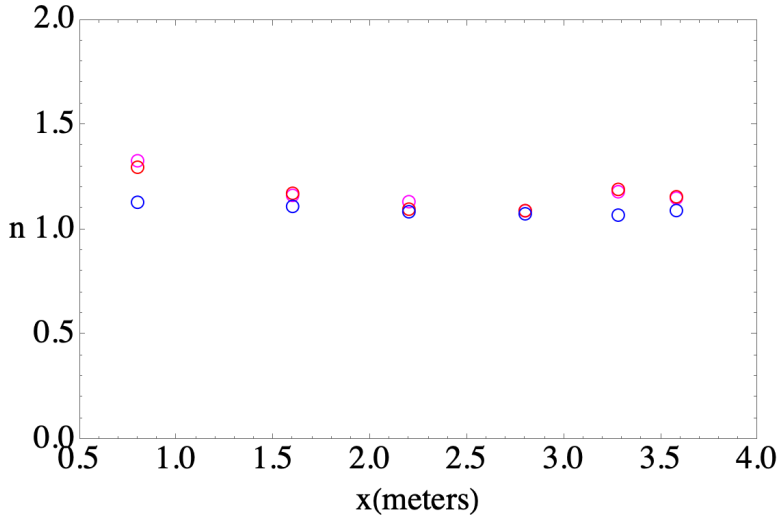

R_e=1.9 ×10^6

R_e=2.8 ×10^6

R_e=3.7 ×10^6

STANFORD
AERONAUTICS &
ASTRONAUTICS

Parameters for the favorable pressure gradient cases

TABLE III. Run data, Reynolds number, optimal model parameters, and RMS error for favorable pressure gradient boundary layer datasets from Jones *et al.*[28] Converging channel entry velocities are $u_0 = 5.0, 7.5$ and 10.0 m/s. Channel half height thickness for these data are at $u = 0.996u_e$; $\delta_h = \delta_{0.996}$. Kinematic viscosity is $\nu = 1.51 \times 10^{-5}\text{m/s}^2$. Note, according to Jones *et al.*,[28] $u_e/u_0 = 1/(1 - x/L)$ and the calibrated sink length is $L = 5.60$m.

$K \times 10^7$	x (mm)	$u_0\left(\frac{\text{m}}{\text{s}}\right)$	R_{δ_1}	R_{δ_2}	$-\beta$	$-\beta_c$	$R_{\delta_{996}}$	R_τ	$\left(\frac{u_e}{u_\tau}\right)$	k	a	m	b	n	$u^+{}_{rms}$
5.39	800	5.0	1112	780	0.2436	0.4145	8656	429	20.16	0.4686	26.88	1.2136	0.3931	1.3295	0.098
5.39	1600	5.0	1629	1192	0.3780	0.6548	14 130	681	20.75	0.4630	25.58	1.2408	0.5284	1.1644	0.068
5.39	2200	5.0	1648	1209	0.3880	0.6726	14 806	709	20.90	0.4670	27.89	1.0869	0.5806	1.1343	0.105
5.39	2800	5.0	1946	1449	0.4713	0.8222	18 244	861	21.20	0.4555	26.89	1.1196	0.6934	1.0908	0.089
5.39	3280	5.0	2138	1606	0.5276	0.9241	20 549	960	21.40	0.4445	26.04	1.1563	0.6831	1.1818	0.067
5.39	3580	5.0	2226	1687	0.5500	0.9671	22 468	1049	21.41	0.4448	25.96	1.1920	0.8189	1.1514	0.068
3.59	800	7.5	1496	1069	0.3613	0.4125	11 752	555	21.17	0.4602	26.62	1.1906	0.3738	1.2986	0.092
3.59	1600	7.5	2000	1470	0.3382	0.5868	17 325	798	21.70	0.4644	28.91	1.0413	0.4647	1.1745	0.085
3.59	2200	7.5	2350	1755	0.4030	0.7040	21 366	977	21.86	0.4557	27.30	1.0822	0.5752	1.0988	0.060
3.59	2800	7.5	2827	2155	0.4850	0.8748	27 899	1262	22.12	0.4431	26.19	1.1527	0.7463	1.0917	0.065
3.59	3280	7.5	2928	2245	0.5202	0.9191	29 762	1338	22.25	0.4374	25.93	1.1726	0.7271	1.1931	0.055
3.59	3580	7.5	3027	2339	0.5344	0.9473	32 204	1452	22.17	0.4403	25.78	1.2037	0.8700	1.1579	0.062
2.70	800	10.0	1862	1343	0.3161	0.4092	15 001	690	21.74	0.4564	28.35	1.0045	0.4324	1.1316	0.097
2.70	1600	10.0	2555	1904	0.3421	0.5969	22 546	1013	22.27	0.4529	27.56	1.0538	0.5090	1.1120	0.074
2.70	2200	10.0	2873	2160	0.3908	0.6846	26 114	1164	22.44	0.4525	26.90	1.0669	0.5491	1.0864	0.047
2.70	2800	10.0	3372	2577	0.4689	0.8273	32 769	1444	22.70	0.4402	25.79	1.1307	0.6833	1.0766	0.047
2.70	3280	10.0	3725	2851	0.5297	0.9351	35 899	1564	22.95	0.4364	25.45	1.1227	0.6653	1.0704	0.073
2.70	3580	10.0	3936	3044	0.5575	0.9888	39 990	1746	22.91	0.4368	25.31	1.1607	0.7504	1.0923	0.095

A modified Clauser pressure gradient parameter

Begin with the von Kármán boundary layer integral equation

$$\frac{d\delta_2}{dx} + (2\delta_2 + \delta_1)\frac{1}{u_e}\frac{du_e}{dx} - \left(\frac{u_\tau}{u_e}\right)^2 = 0$$

The function $u_e(x)$ is the free stream velocity and the friction velocity is

$$u_\tau(x) \equiv \left(\frac{\tau_w}{\rho}\right)^{1/2}$$

The displacement thickness is defined as

$$\delta_1(x) = \int_0^\delta \left(1 - \frac{u}{u_e}\right) dy$$

The momentum thickness is

$$\delta_2(x) = \int_0^\delta \frac{u}{u_e}\left(1 - \frac{u}{u_e}\right) dy$$

Assume potential flow about a body in a free stream at a reference velocity U_∞.

$$U = \frac{u_e(x)}{U_\infty}$$

And a Reynolds number based on the distance x from the origin of the flow.

$$R_x = \frac{U_\infty x}{\nu}$$

Express the Kármán equation in terms of displacement and momentum thickness Reynolds numbers

$$\frac{d\delta_2}{dx} + (2\delta_2 + \delta_1)\frac{1}{u_e}\frac{du_e}{dx} - \left(\frac{u_\tau}{u_e}\right)^2 = 0 \qquad \frac{d(\delta_2 u_e)}{dx} = u_e\frac{d\delta_2}{dx} + \delta_2\frac{du_e}{dx}$$

$$\frac{d(\delta_2 u_e)}{dx} + (\delta_2 + \delta_1)\frac{du_e}{dx} - u_e\left(\frac{u_\tau}{u_e}\right)^2 = 0$$

$$R_{\delta_1} = \frac{\delta_1 u_e}{\nu} \qquad R_{\delta_2} = \frac{\delta_2 u_e}{\nu} \qquad R_x = \frac{x u_\infty}{\nu} \qquad U = \frac{u_e}{U_\infty}$$

$$\frac{dR_{\delta_2}}{dR_x} + (R_{\delta_2} + R_{\delta_1})\frac{1}{U}\frac{dU}{dR_x} - U\left(\frac{u_\tau}{u_e}\right)^2 = 0$$

$$\frac{dR_{\delta_2}}{dR_x} = U\left(\frac{u_\tau}{u_e}\right)^2\left(1 - \frac{(R_{\delta_2} + R_{\delta_1})}{\left(\frac{u_\tau}{u_e}\right)^2}\frac{1}{U^2}\frac{dU}{dR_x}\right)$$

$$\frac{dR_\tau}{dR_x} = \frac{U}{dR_{\delta_2}/dR_\tau}\left(\frac{u_\tau}{u_e}\right)^2\left(1 - \frac{(R_{\delta_2} + R_{\delta_1})}{\left(\frac{u_\tau}{u_e}\right)^2}\frac{1}{U^2}\frac{dU}{dR_x}\right)$$

Define the following functions

The boundary layer friction law

$$\frac{u_e}{u_\tau} = \int_0^{R_\tau} \frac{2\left(1 - \frac{s}{R_\tau}\right)}{1 + \left(1 + 4\lambda^2\left(1 - \frac{s}{R_\tau}\right)\right)^{1/2}} ds \equiv F_0$$

Displacement thickness Reynolds number in wall units

$$R_{\delta_1} = \frac{u_e \delta_1}{\nu} = \frac{u_e}{u_\tau} \int_0^{R_\tau} \left(1 - \frac{u_\tau}{u_e} u^+\right) dy^+ \equiv F_1$$

Momentum thickness Reynolds number in wall units

$$R_{\delta_2} = \frac{u_e \delta_2}{\nu} = \int_0^{R_\tau} u^+ \left(1 - \frac{u_\tau}{u_e} u^+\right) dy^+ \equiv F_2$$

Derivative of the momentum thickness Reynolds number in wall units

$$\frac{dF_2}{dR_\tau} \equiv F_3$$

Express the Kármán equation as an equation for the friction Reynolds number as a function of streamwise Reynolds number.

$$\frac{dR_\tau}{dR_x} = \frac{U}{dR_{\delta_2}/dR_\tau}\left(\frac{u_\tau}{u_e}\right)^2\left(1 - \frac{(R_{\delta_2} + R_{\delta_1})}{\left(\frac{u_\tau}{u_e}\right)^2}\frac{1}{U^2}\frac{dU}{dR_x}\right)$$

$$\boxed{\frac{dR_\tau}{dR_x} = \frac{U}{{F_0}^2 F_3}\left(1 - {F_0}^2(F_2 + F_1)\frac{1}{U^2}\frac{dU}{dR_x}\right)}$$

$$\frac{dF_2}{dR_\tau} \equiv F_3$$

The logical choice for the modified Clauser parameter is

$$\boxed{\beta_c = -{F_0}^2(F_2 + F_1)\frac{1}{U^2}\frac{dU}{dR_x}}$$

Deconstruct the modified Clauser parameter

$$\beta_c = -{F_0}^2(F_2 + F_1)\frac{1}{U^2}\frac{dU}{dR_x}$$

$$\beta_c = \left(\frac{u_e}{u_\tau}\right)^2 \frac{u_e}{\nu}\frac{U_\infty}{u_e}(\delta_2 + \delta_1)\frac{\nu}{U_\infty}\frac{1}{u_e}\frac{du_e}{dx}$$

$$\beta_c = \left(\frac{1}{u_\tau}\right)^2 (\delta_2 + \delta_1)u_e\frac{du_e}{dx}$$

$$\boxed{\beta_c = \rho\frac{(\delta_2 + \delta_1)}{\tau_w}\frac{dp_e}{dx}}$$

The usual definition is

$$\beta = \rho\frac{\delta_1}{\tau_w}\frac{dp_e}{dx}$$

The UVP wake parameters b and n are related through β_c independent of R_τ

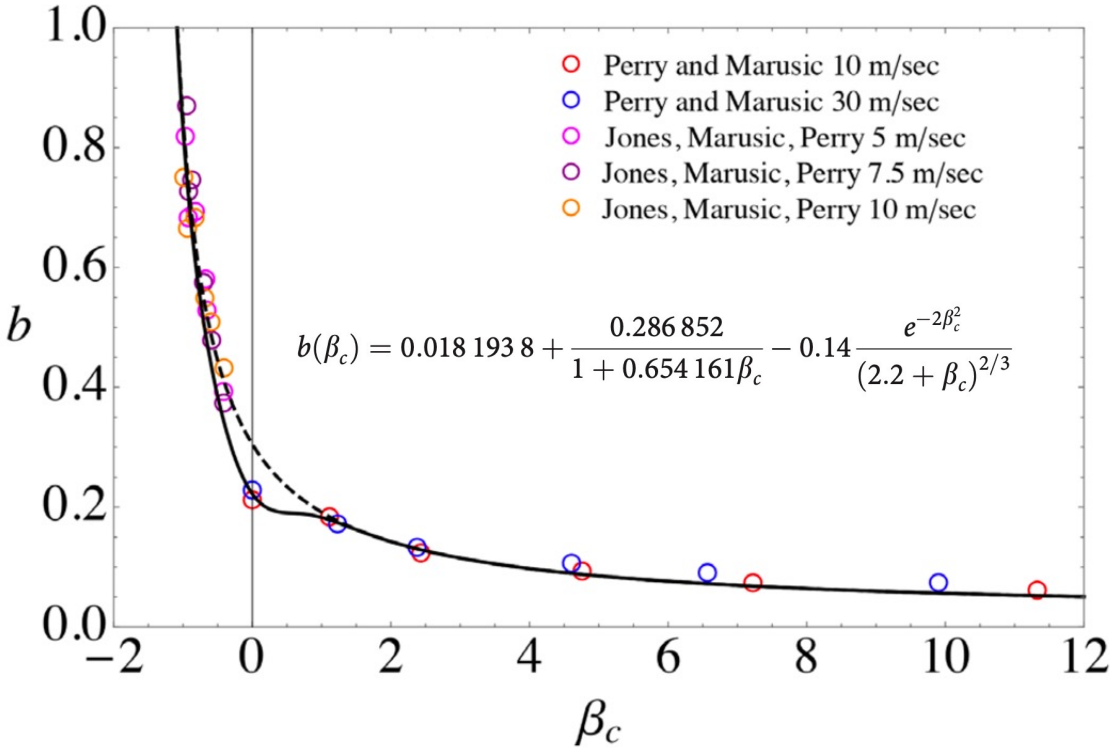

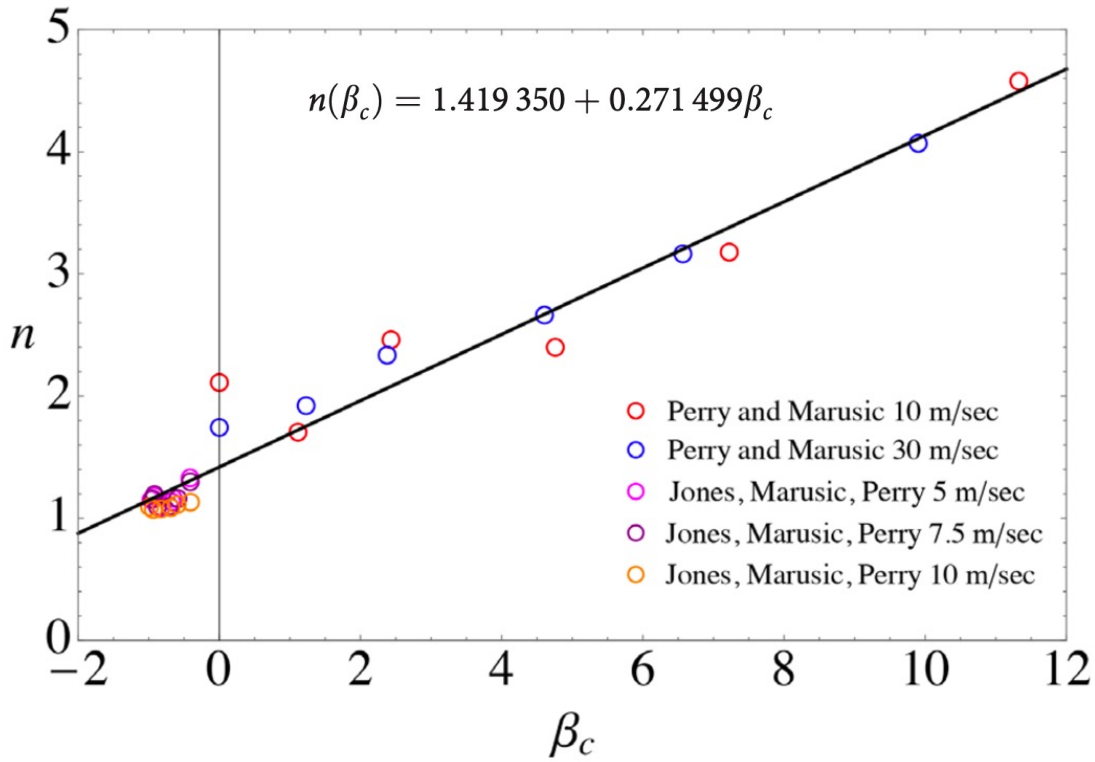

High Reynolds number

Turbulent boundary layer wall variables y^+ and u^+ and the friction Reynolds number R_τ

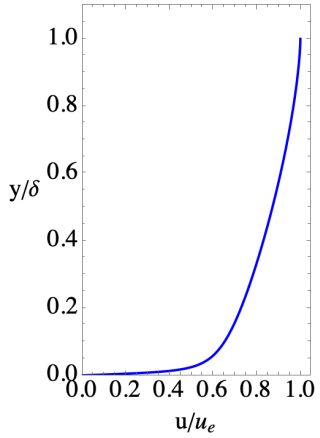

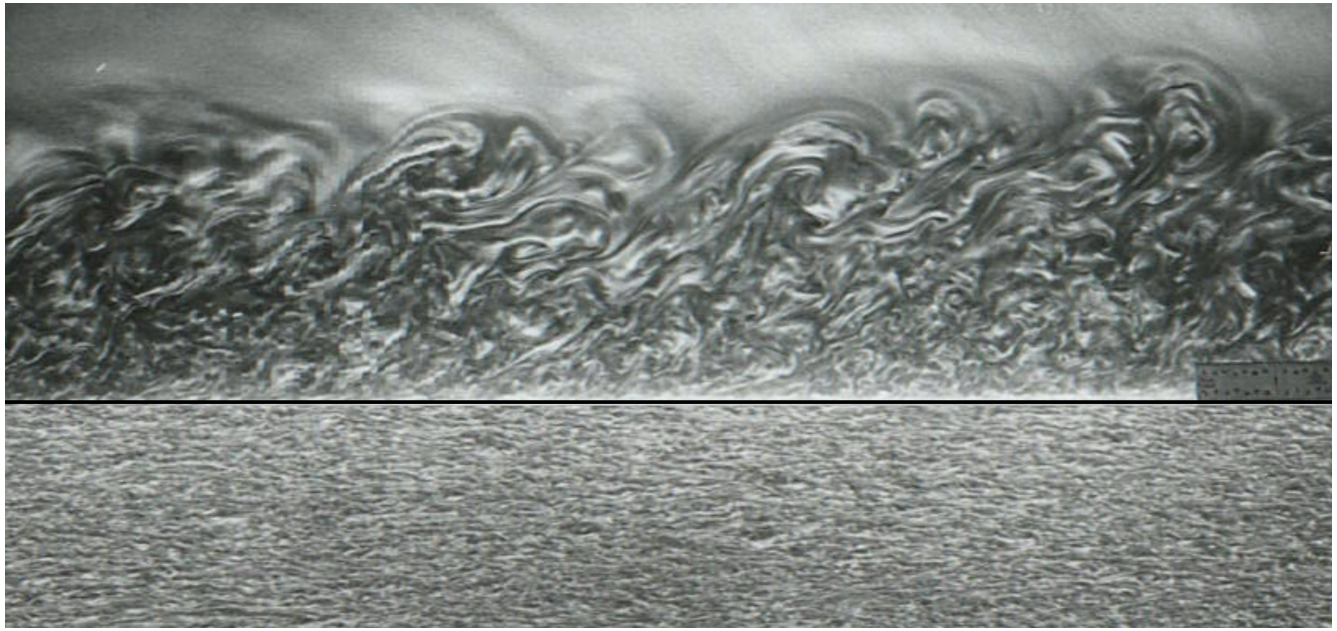

$$\tau_w = \mu \left.\frac{\partial U}{\partial y}\right|_{y=0} \qquad u_\tau = \sqrt{\frac{\tau_w}{\rho}}$$

$$y^+ = \frac{y u_\tau}{\nu} \qquad u^+ = \frac{u}{u_\tau}$$

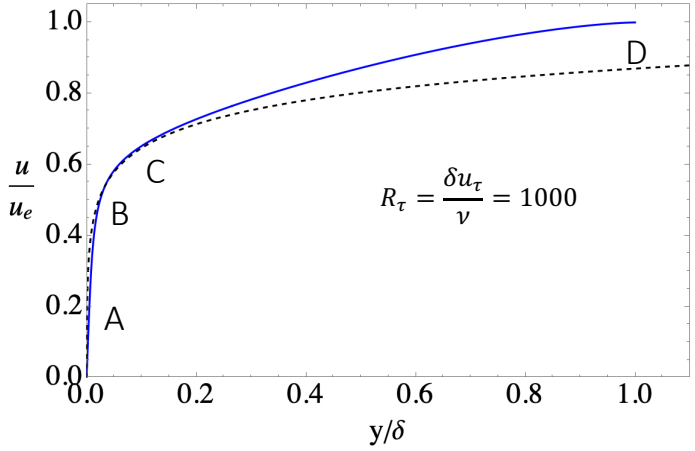

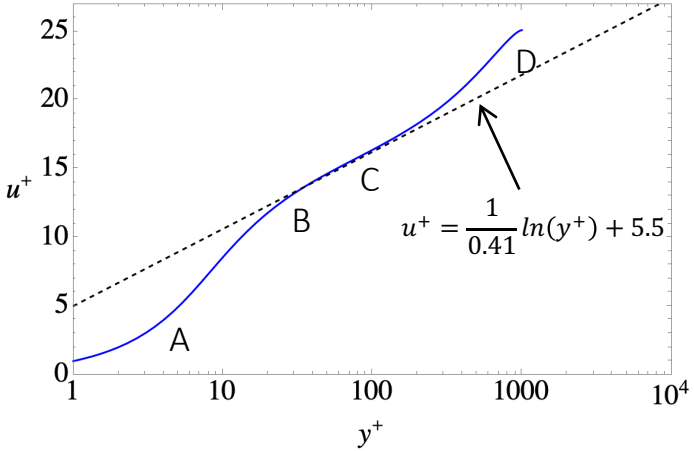

$$R_\tau = \frac{\delta u_\tau}{\nu} = \delta^+$$

$$\frac{y}{\delta} = \frac{y^+}{R_\tau}$$

Recall the UVP

$$u^+(k,a,m,b,n,R_\tau,y^+) = \int_0^{y^+} \frac{2\left(1-\frac{s}{R_\tau}\right)}{1+\left(1+4\lambda^2\left(1-\frac{s}{R_\tau}\right)\right)^{1/2}} ds$$

$$\lambda(k,a,m,b,n,R_\tau,y^+) = \frac{ky^+(1-e^{-(y^+/a)^m})}{\left(1+\left(\frac{y^+}{bR_\tau}\right)^n\right)^{1/n}}$$

Carry out a scaling - Multiply and divide the damping and wake terms by *k*

Modified wall-wake mixing length function. The parameters *k* and *a* become one parameter *ka*.

$$\lambda(k,a,m,b,n,R_\tau,y^+) = \frac{ky^+(1-e^{-(y^+/a)^m})}{\left(1+\left(\frac{y^+}{bR_\tau}\right)^n\right)^{1/n}} = \frac{ky^+(1-e^{-(ky^+/ka)^m})}{\left(1+\left(\frac{ky^+}{bkR_\tau}\right)^n\right)^{1/n}} = \tilde{\lambda}(ka,m,b,n,kR_\tau,ky^+)$$

Scaled velocity profile

$$ku^+(ka,m,b,n,kR_\tau,ky^+) = \int_0^{ky^+} \frac{2\left(1-\frac{s}{kR_\tau}\right)}{1+\left(1+4\tilde{\lambda}^2\left(1-\frac{s}{kR_\tau}\right)\right)^{1/2}} ds$$

$$y^+ \rightarrow ky^+$$

$$R_\tau \rightarrow kR_\tau$$

$$u/u_\tau \rightarrow ku/u_\tau$$

Define the shape function

$$\Phi(ka, m, b, n, kR_\tau, ky^+) = \int_0^{ky^+} \frac{2\left(1 - \frac{s}{kR_\tau}\right)}{1 + \left(1 + 4\tilde{\lambda}^2\left(1 - \frac{s}{kR_\tau}\right)\right)^{1/2}} ds - ln(ky^+)$$

Note $\quad ky^+ = \left(\frac{y}{\delta_h}\right) kR_\tau$

Fix y/δ_h and plot Φ versus kR_τ

Above $kR_\tau \cong 2000$, Φ *is independent of* R_τ

$$\Phi(ka, m, b, n, kR_\tau, ky^+) = \phi\left(ka, m, b, n, \frac{y}{\delta_h}\right)$$

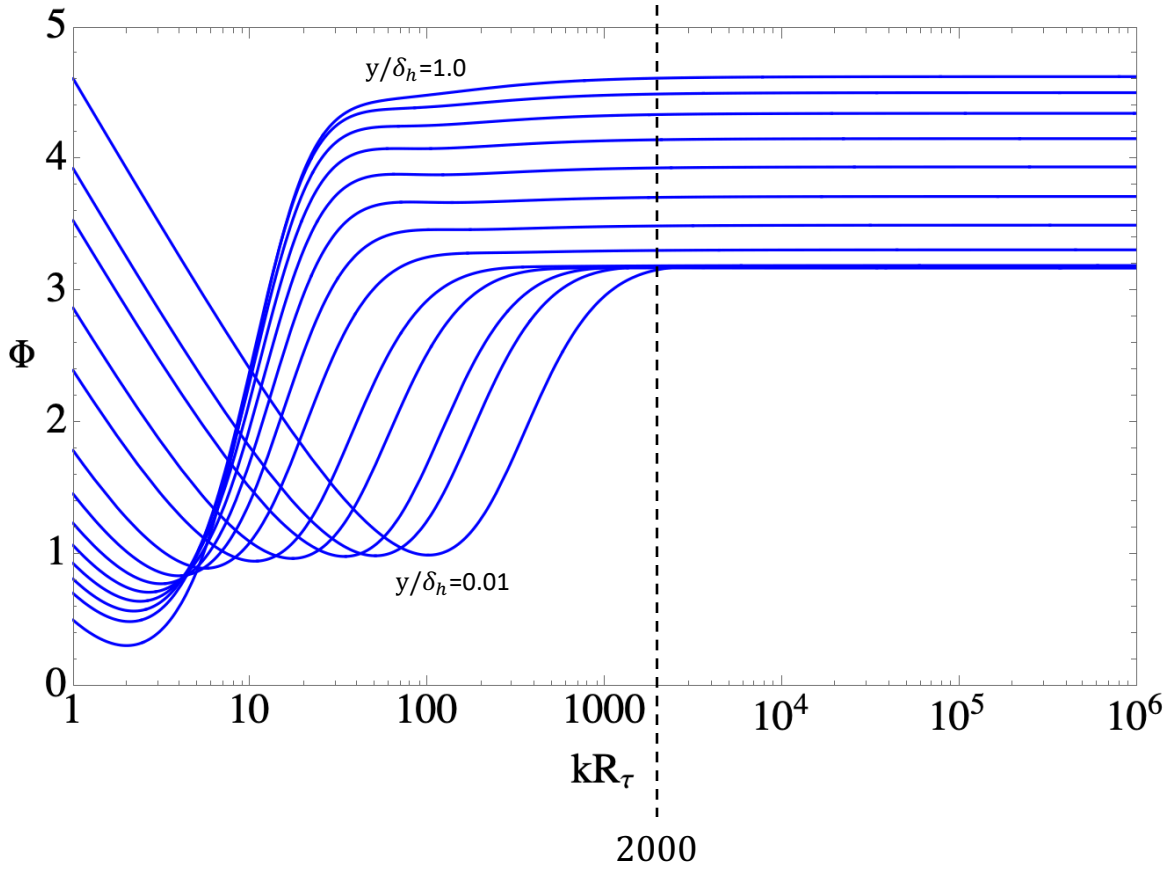

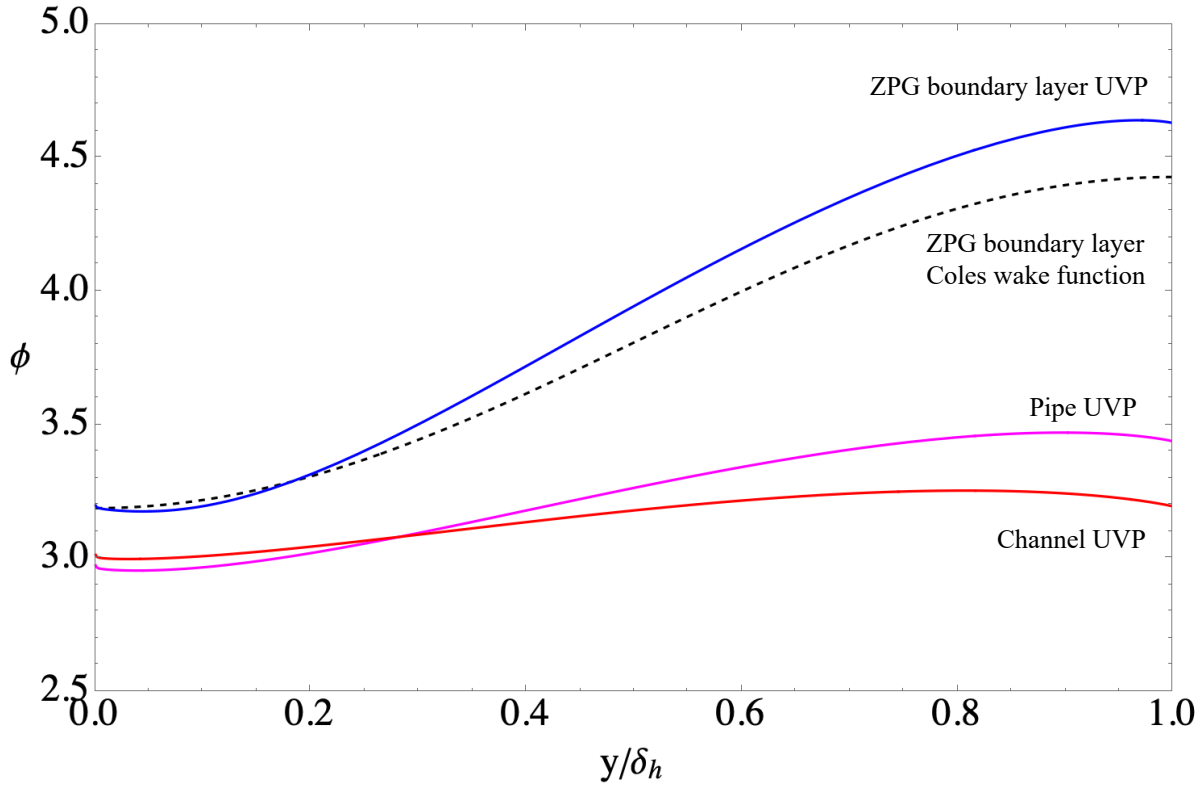

Explicit high Reynolds number form of the UVP

$$u^+(k,a,m,b,n,R_\tau,y^+) = \int_0^{y^+} \frac{2\left(1-\frac{s}{R_\tau}\right)}{1+\left(1+4\lambda^2\left(1-\frac{s}{R_\tau}\right)\right)^{1/2}} ds$$

$0 < y^+ < R_\tau$

At Reynolds numbers larger than $kR_\tau \cong 2000$ the boundary layer velocity profile above $y^+ = 132$ is accurately approximated by

$$u^+ = \frac{1}{k} ln(ky^+) + \frac{1}{k}\phi\left(ka, m, b, n, \frac{y}{\delta_h}\right)$$

$y^+ > 132$

Evaluate at the boundary layer edge to determine the friction law.

$$\frac{u_e}{u_\tau} = \frac{1}{k} ln(kR_\tau) + \frac{1}{k}\phi\left(ka, m, b, n, 1\right)$$

STANFORD
AERONAUTICS &
ASTRONAUTICS

In the shape function ϕ for boundary layers, the parameters *b* and *n* are determined by β_c

$$u^+ = \frac{1}{k} ln(ky^+) + \frac{1}{k}\phi\left(ka, m, \beta_c, \frac{y}{\delta_h}\right)$$

$y^+ > 132$
$kR_\tau > 2000$

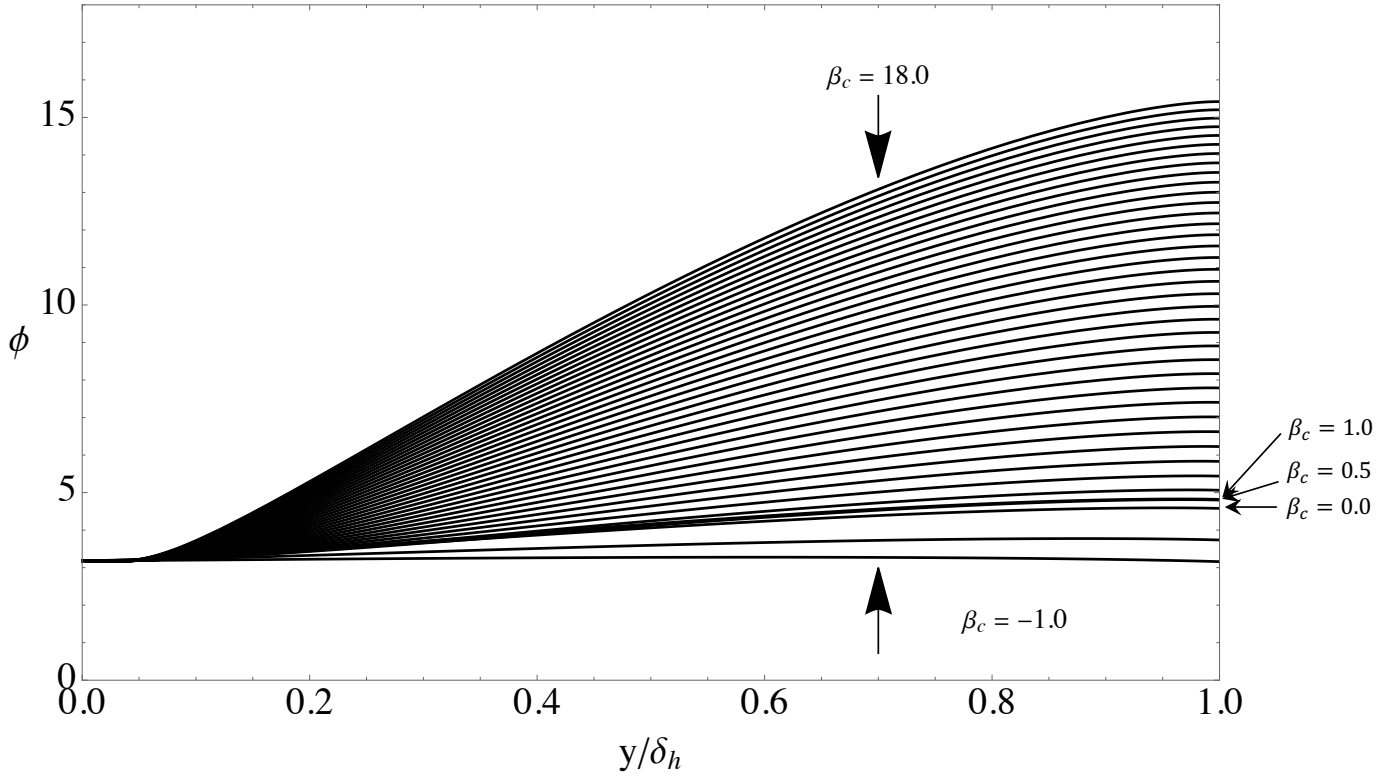

The shape function is accurately approximated by a bivariate polynomial in β_c and y/δ_h.

In the presence of a pressure gradient, the wall parameters (*k, a, m*) are kept constant at the ZPG boundary layer values while the wake parameters (*b, n*) are treated as functions of β_c using the correlations. The figure at the right shows the shape function for a range of values of β_c. Changes in ϕ with β_c are smooth and monotonic. A polynomial of high order is a safe, reliable fit in this situation since there is no question of y/δ_h falling outside of the range $0 \le y/\delta_h \le 1$. The family of shape functions shown in the Figure is accurately approximated by an eighth-order polynomial.

$$\phi\left(\beta_c, \frac{y}{\delta_h}\right) = c_0(\beta_c) + c_1(\beta_c)\left(\frac{y}{\delta_h}\right) + c_2(\beta_c)\left(\frac{y}{\delta_h}\right)^2 + c_3(\beta_c)\left(\frac{y}{\delta_h}\right)^3 + c_4(\beta_c)\left(\frac{y}{\delta_h}\right)^4 + c_5(\beta_c)\left(\frac{y}{\delta_h}\right)^5 + c_6(\beta_c)\left(\frac{y}{\delta_h}\right)^6 + c_7(\beta_c)\left(\frac{y}{\delta_h}\right)^7 + c_8(\beta_c)\left(\frac{y}{\delta_h}\right)^8$$

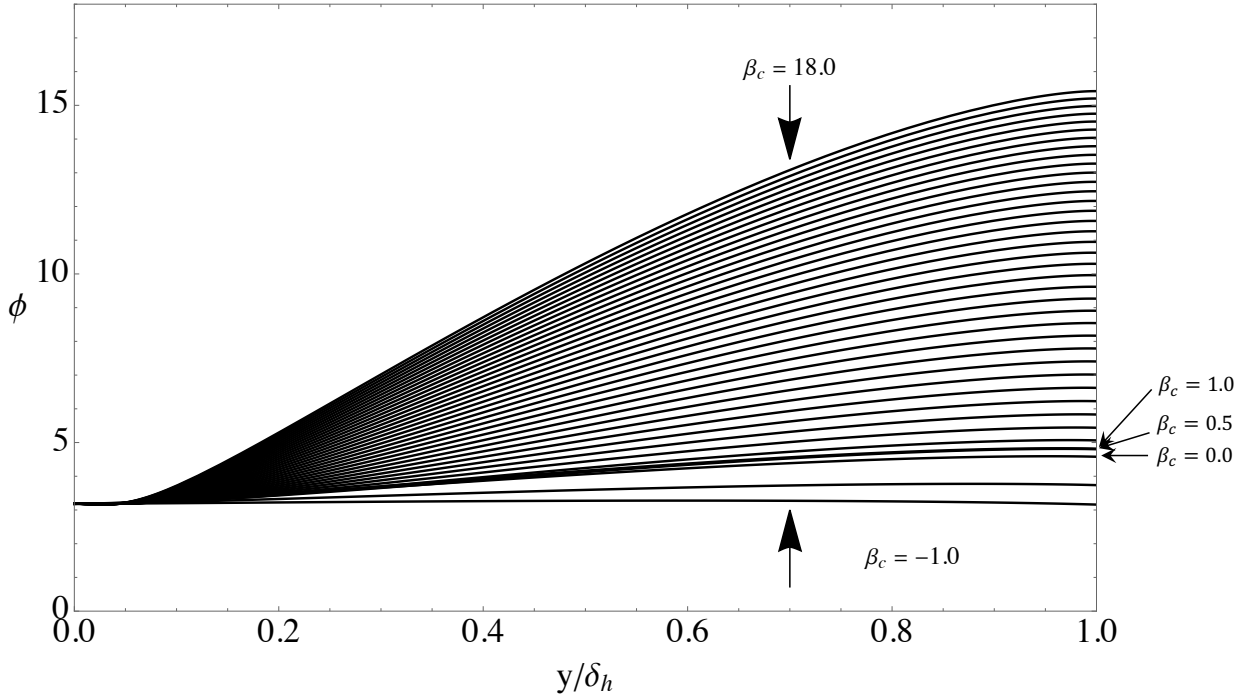

It is important to note that $\phi(\beta_c, y/\delta_h)$ is universal in the sense that it applies to any pressure gradient wall flow that falls in the range -1 < β_c < 18. Higher order fits could be used to increase the range of β_c beyond 18.0.

With $\phi(ka, m, \beta_c, y/\delta_h)$ known explicitly as a bivariate polynomial, the displacement thickness and momentum thickness integrals can be carried out up to whatever R_τ is required. This leads to polynomial expressions for the friction and thickness functions $F_0(\beta_c, R_\tau)$, $F_1(\beta_c, R_\tau)$, $F_2(\beta_c, R_\tau)$ and $F_3(\beta_c, R_\tau)$. Once these functions are known, the UVP integral method no longer requires the computation of nested integrals. As a result, the time to calculate a solution of the Karman integral equation is independent of the Reynolds number. The viscous drag coefficient for any chord Reynolds number airfoil can be determined in a few seconds. Above about R_{chord} = 10^6, the explicit UVP method matches the results using the integral form of the UVP almost exactly.

STANFORD
AERONAUTICS &
ASTRONAUTICS

The coefficients $c_0(\beta_c)$ to $c_8(\beta_c)$ are approximated by tenth-order polynomial functions of the pressure gradient parameter β_c and are strictly limited to the range $-1 < \beta_c < 18$ indicated in the Figure. The expressions for $c_0(\beta_c)$ to $c_8(\beta_c)$ are provided to the right.

It is important to note that $\phi(\beta_c, y/\delta_h)$ is universal in the sense that it applies to any pressure gradient wall flow that falls in the range $-1 < \beta_c < 18$. Higher order fits could be used to increase the range of β_c beyond 18.0.

$$\phi\left(\beta_c, \frac{y}{\delta_h}\right) = c_0(\beta_c) + c_1(\beta_c)\left(\frac{y}{\delta_h}\right) + c_2(\beta_c)\left(\frac{y}{\delta_h}\right)^2 + c_3(\beta_c)\left(\frac{y}{\delta_h}\right)^3 + c_4(\beta_c)\left(\frac{y}{\delta_h}\right)^4 + c_5(\beta_c)\left(\frac{y}{\delta_h}\right)^5 + c_6(\beta_c)\left(\frac{y}{\delta_h}\right)^6 + c_7(\beta_c)\left(\frac{y}{\delta_h}\right)^7 + c_8(\beta_c)\left(\frac{y}{\delta_h}\right)^8$$

$$\begin{aligned} c_0(\beta_c) = {} & 3.185\,213\,759\,059\,279\,5 - 0.000\,097\,351\,124\,875\,088\,01\ \beta_c \\ & + 0.000\,857\,641\,541\,537\,847\,5\ \beta_c^2 \\ & - 0.000\,134\,299\,418\,144\,835\,46\ \beta_c^3 \\ & - 0.000\,020\,654\,101\,916\,920\,754\ \beta_c^4 \\ & + 0.000\,015\,020\,911\,822\,593\,57\ \beta_c^5 \\ & - 2.968\,623\,256\,456\,977 \times 10^{-6}\ \beta_c^6 \\ & + 2.963\,701\,061\,289\,852\,4 \times 10^{-7}\ \beta_c^7 \\ & - 1.631\,850\,736\,220\,117\,2 \times 10^{-8}\ \beta_c^8 \\ & + 4.735\,140\,769\,133\,537 \times 10^{-10}\ \beta_c^9 \\ & - 5.670\,359\,008\,088\,255\,5 \times 10^{-12}\ \beta_c^{10}, \end{aligned} \quad \text{(A1)}$$

$$\begin{aligned} c_1(\beta_c) = {} & 0.177\,875\,635\,158\,609\,52 - 0.243\,068\,542\,472\,120\,7\ \beta_c \\ & - 0.182\,315\,590\,796\,708\,98\ \beta_c^2 \\ & + 0.114\,167\,281\,428\,819\,74\ \beta_c^3 \\ & - 0.032\,508\,461\,93\,233\,937\ \beta_c^4 \\ & + 0.004\,881\,950\,187\,888\,647\ \beta_c^5 \\ & - 0.000\,419\,972\,498\,600\,616\,4\ \beta_c^6 \\ & + 0.000\,020\,756\,027\,245\,732\,183\ \beta_c^7 \\ & - 5.360\,810\,884\,925\,711 \times 10^{-7}\ \beta_c^8 \\ & + 4.864\,234\,131\,520\,179\,6 \times 10^{-9}\ \beta_c^9 \\ & + 2.745\,541\,114\,505\,071 \times 10^{-11}\ \beta_c^{10}, \end{aligned} \quad \text{(A2)}$$

$$\begin{aligned} c_2(\beta_c) = {} & 8.752\,630\,174\,726\,951 + 5.383\,284\,010\,214\,323\ \beta_c \\ & - 1.802\,896\,664\,601\,566\,7\ \beta_c^2 - 0.077\,034\,046\,540\,169\,49\ \beta_c^3 \\ & + 0.335\,381\,660\,158\,488\,7\ \beta_c^4 - 0.103\,409\,008\,148\,911\,44\ \beta_c^5 \\ & + 0.015\,699\,101\,594\,675\,673\ \beta_c^6 \\ & - 0.001\,372\,392\,667\,304\,845\,8\ \beta_c^7 \\ & + 0.000\,070\,043\,102\,706\,461\ \beta_c^8 \\ & - 1.940\,086\,907\,438\,102\,7 \times 10^{-6}\ \beta_c^9 \\ & + 2.254\,603\,431\,206\,475\,2 \times 10^{-8}\ \beta_c^{10}, \end{aligned} \quad \text{(A3)}$$

$$\begin{aligned} c_3(\beta_c) = {} & -29.320\,201\,478\,527\,7 - 13.009\,083\,141\,290\,633\ \beta_c \\ & + 9.891\,072\,103\,799\,035\ \beta_c^2 + 0.286\,430\,751\,940\,286\,4\ \beta_c^3 \\ & - 1.264\,366\,997\,570\,824\ \beta_c^4 + 0.357\,951\,024\,377\,768\,16\ \beta_c^5 \\ & - 0.051\,953\,118\,683\,825\,3\ \beta_c^6 \\ & + 0.004\,449\,565\,462\,995\,644\ \beta_c^7 \\ & - 0.000\,225\,332\,996\,880\,537\,36\ \beta_c^8 \\ & + 6.231\,250\,458\,034\,746 \times 10^{-6}\ \beta_c^9 \\ & - 7.250\,246\,433\,619\,231 \times 10^{-8}\ \beta_c^{10}, \end{aligned} \quad \text{(A4)}$$

$$\begin{aligned} c_4(\beta_c) = {} & 63.370\,268\,858\,329\,155 + 21.206\,924\,878\,802\,89\ \beta_c \\ & - 28.490\,362\,428\,461\,17\ \beta_c^2 - 1.383\,788\,687\,404\,143\,2\ \beta_c^3 \\ & + 2.999\,048\,905\,796\,227\,5\ \beta_c^4 - 0.761\,144\,546\,069\,162\,7\ \beta_c^5 \\ & + 0.104\,860\,072\,527\,180\,98\ \beta_c^6 \\ & - 0.008\,803\,651\,704\,295\,447\ \beta_c^7 \\ & + 0.000\,444\,105\,810\,851\,922\,5\ \beta_c^8 \\ & - 0.000\,012\,319\,542\,850\,362\,865\ \beta_c^9 \\ & + 1.441\,663\,408\,041\,264\,3 \times 10^{-7}\ \beta_c^{10}, \end{aligned} \quad \text{(A5)}$$

$$\begin{aligned} c_5(\beta_c) = {} & -87.693\,764\,826\,178\,6 - 22.352\,131\,224\,850\,766\ \beta_c \\ & + 47.942\,643\,158\,529\,59\ \beta_c^2 + 3.144\,148\,516\,656\,517\ \beta_c^3 \\ & - 4.414\,688\,172\,210\,721\ \beta_c^4 + 1.011\,217\,929\,468\,684\,7\ \beta_c^5 \\ & - 0.132\,607\,179\,383\,751\,05\ \beta_c^6 \\ & + 0.010\,971\,698\,041\,512\,124\ \beta_c^7 \\ & - 0.000\,554\,916\,304\,796\,180\,4\ \beta_c^8 \\ & + 0.000\,015\,534\,289\,801\,032\,056\ \beta_c^9 \\ & - 1.837\,286\,959\,416\,604\,7 \times 10^{-7}\ \beta_c^{10}, \end{aligned} \quad \text{(A6)}$$

$$\begin{aligned} c_6(\beta_c) = {} & 70.968\,812\,707\,064\,7 + 12.583\,124\,149\,174\,417\ \beta_c \\ & - 46.888\,434\,832\,647\,61\ \beta_c^2 - 3.734\,105\,839\,184\,008\,5\ \beta_c^3 \\ & + 3.884\,301\,374\,624\,679\ \beta_c^4 - 0.802\,627\,524\,234\,329\,7\ \beta_c^5 \\ & + 0.099\,762\,336\,519\,354\,65\ \beta_c^6 \\ & - 0.008\,144\,173\,595\,693\,59\ \beta_c^7 \\ & + 0.000\,414\,872\,495\,566123\,67\ \beta_c^8 \\ & - 0.000\,011\,778\,008\,804\,226\,057\ \beta_c^9 \\ & + 1.413\,661\,707\,265\,926\,8 \times 10^{-7}\ \beta_c^{10}, \end{aligned} \quad \text{(A7)}$$

$$\begin{aligned} c_7(\beta_c) = {} & -29.738\,042\,179\,000\,644 - 2.266\,916\,912\,193\,806\ \beta_c \\ & + 24.689\,251\,860\,732\,828\ \beta_c^2 + 2.271\,539\,156\,916\,986\ \beta_c^3 \\ & - 1.867\,706\,886\,189\,081\,3\ \beta_c^4 + 0.344\,688\,708\,245\,448\,8\ \beta_c^5 \\ & - 0.040\,023\,433\,517\,290\,326\ \beta_c^6 \\ & + 0.003\,211\,634\,372\,538\,153\ \beta_c^7 \\ & - 0.000\,165\,444\,382\,500\,483\,54\ \beta_c^8 \\ & + 4.791\,043\,532\,302\,556 \times 10^{-6}\ \beta_c^9 \\ & - 5.865\,386\,244\,138\,967\,5 \times 10^{-8}\ \beta_c^{10}, \end{aligned} \quad \text{(A8)}$$

$$\begin{aligned} c_8(\beta_c) = {} & 4.625\,148\,665\,477\,973 - 0.505\,275\,164\,231\,022\,5\ \beta_c \\ & - 5.397\,029\,748\,250\,34\ \beta_c^2 - 0.562\,142\,236\,631\,621\,3\ \beta_c^3 \\ & + 0.375\,511\,158\,572\,171\,93\ \beta_c^4 - 0.060\,255\,387\,771\,924\,11\ \beta_c^5 \\ & + 0.006\,292\,183\,567\,809\,945\ \beta_c^6 \\ & - 0.000\,488\,834\,388\,113\,832\,5\ \beta_c^7 \\ & + 0.000\,025\,608\,788\,685\,571\,06\ \beta_c^8 \\ & - 7.651\,119\,404\,966\,455 \times 10^{-7}\ \beta_c^9 \\ & + 9.652\,853\,992\,263\,516 \times 10^{-9}\ \beta_c^{10}. \end{aligned} \quad \text{(A9)}$$

Conclusions

1)The UVP provides a useful replacement of the classical wall-wake profile and can be applied to a wide range of wall-bounded flows. The profile is uniformly valid from the wall to the free stream at all Reynolds numbers. At low Reynolds number, laminar to turbulent transition is that of a fully tripped flow.

2) At Reynolds numbers larger than $kR_\tau \cong 2000$, above the buffer layer (about y+ = 132), the UVP accurately approximates an explicit form.

$$u^+ = \frac{1}{k} ln(ky^+) + \frac{1}{k}\phi\left(ka, m, \beta_c, \frac{y}{\delta_h}\right)$$

3) The inherent dependence of the UVP on Reynolds number, extended to include the effect of pressure gradient, enables it to be used as the basis of a new method for integrating the Karman equation for a wide variety of attached, wall bounded flows. An example will be presented in Lecture 2.

4) There is no limit to the Reynolds number that can be computed suggesting that the UVP can be applied to very large scale aerodynamic, hydrodynamic and geophysical flows.

5) The minimization process is not convex. Alternate values of the model parameters, particularly k and a can lead to the same degree of accuracy. This is the case at low and moderate Reynolds numbers but at high Reynolds numbers alternate minima appear to be close together.

Ultimately fundamental questions about the optimal parameters will need to be answered as to their uniqueness at high Reynolds number, their numerical values, their dependence on flow geometry and their possible weak dependence on Reynolds number, free stream turbulence, surface roughness, Mach number and so forth.

STANFORD
AERONAUTICS &
ASTRONAUTICS

Main References

Coles, D.E. 1956 The law of the wake in the turbulent boundary layer. *J. Fluid Mech.* 1 (2), 191–226.

Prandtl, L. 1934 *Aerodynamic Theory* (ed. W. F. Durand), vol III, chap. 21, p. 134. Julius Springer.

Cantwell, B.J. 2019 A universal velocity profile for smooth wall pipe flow. *J. Fluid Mech.* 878, 834–874.

Spalding, B.D. 1961 A single formula for the 'law of the wall'. *Trans. ASME J. Appl. Mech.* 0, 455–458.

Cantwell, B.J. 2021 Integral measures of the zero pressure gradient boundary layer over the Reynolds number range $0 \leq R_T < \infty$. *Phys. Fluids* 33, 085108.

M. A. Subrahmanyam, B. J. Cantwell, and J. J. Alonso, "A universal velocity profile for turbulent wall flows including adverse pressure gradient boundary layers,"JFM. 933, A16 (2022).

She, Z.-S., Chen X. & Hussain, F. 2017 Quantifying wall turbulence via a symmetry approach: a lie group theory. *J. Fluid Mech.* 827, 322–356.

Chen, X., Hussain, F. & She, Z. 2018 Quantifying wall turbulence via a symmetry approach. Part 2. Reynolds stresses. *J. Fluid Mech.* 405, 401–438.

Chen, X. &Sreenivasen, K.R. 2021 Reynolds number scaling of the peak turbulence intensity in wall flows. *J. Fluid Mech.* 908, R3.

van Driest, E.R. 1956 On turbulent flow near a wall. *J. Aeronaut. Sci.* 23 (11), 1007–1011.

Ramis, G.E.-A.Ö. & Schlatter, P. 2014 Simulation and validation of a spatially evolving turbulent boundary layer up to *Re* = 8300. *Intl J. Heat Fluid Flow* 47, 57–69.

Sillero, J.A., Jimenez, J. & Moser, R.D. 2013 One-point statistics for turbulent wall-bounded flows at Reynolds numbers up to δ+ = 2000. *Phys. Fluids* 25 (10), 105102.

Simens, M.P., Jimenez, J., Hoyas, S. & Mizuno, Y. 2009 A high-resolution code for turbulent boundary layers. *J. Comput. Phys.* 228 (11), 4218–4231.

Vinuesa, R., Bobke, A., Örlu, R. & Schlatter, P. 2016 On determining characteristic length scales in pressure-gradient turbulent boundary layers. *Phys. Fluids* 28, 055101.

Yamamoto, Y. & Tsuji, Y. 2018 Numerical evidence of logarithmic regions in channel flow at R_T = 8000. *Phys. Rev. Fluids* 3, 012602.

Zagarola, M.V. 1996 Mean-flow scaling of turbulent pipe flow. Doctoral dissertation, Princeton University.

Zagarola, M.V. & Smits, A.J. 1998 Mean-flow scaling of turbulent pipe flow. *J. Fluid Mech.* 373, 33–79.

McKeon, B.J. 2003 High Reynolds number turbulent pipe flow. Doctoral dissertation, Princeton University.

McKeon, B. J., Li, J., Jiang, W., Morrison, J. F. & Smits, A. J. 2003 Pitot probe corrections in fully developed turbulent pipe flow. *Meas. Sci. Technol.* 14, 1449–1458.

R. Baidya, J. Phillip, N. Hutchins, J. P. Monty, and I. Marusic, "Distance from the wall scaling of turbulent motions in wall-bounded flows," Phys. Fluids 29, 020712 (2017).

A. E. Perry and I. Marusic, "A wall-wake model for the turbulence structure of boundary layers. Part 2. Further experimental support," J. Fluid Mech. 298, 361–407 (1995).

M. Jones, I. Marusic, and A. E. Perry, "Evolution and structure of sink-flow turbulent boundary layers," J. Fluid Mech. 428, 1–27 (2001).